

APPLICATION OF THE EXTENDED PITZER EQUATION TO
NUCLEAR FUEL REPROCESSING

by

Matthew J. Wavada

A thesis submitted to the faculty of
The University of Utah
in partial fulfillment of the requirements for the degree of

Master of Science

Department of Chemical Engineering

The University of Utah

May 2012

Copyright © Matthew J. Wavada 2012

All Rights Reserved

The University of Utah Graduate School

STATEMENT OF THESIS APPROVAL

The thesis of Matthew J. Wavada
has been approved by the following supervisory committee members:

<u>Terry Ring</u>	, Chair	<u>2/29/2012</u> Date Approved
<u>John McLennan</u>	, Member	<u>2/29/2012</u> Date Approved
<u>Geoffrey D. Silcox</u>	, Member	<u>2/29/2012</u> Date Approved

and by JoAnn Lighty, Chair of
the Department of Chemical Engineering

and by Charles A. Wight, Dean of The Graduate School.

ABSTRACT

A rigorous method for calculating the activity coefficients of ions in aqueous solutions during nuclear fuel reprocessing is presented along with predictions of the model during the criticality event that took place on October 17, 1978 at the Idaho Chemical Processing Plant. Determination and validation of the parameters for the extended Pitzer model were performed using OLI database simulations to supplement available experimental data. Values for the parameters for the neutral species uranyl nitrate ($\text{UO}_2(\text{NO}_3)_2$) and nitric acid (HNO_3) from Hlushak et al. were determined to accurately predict the activity coefficients of these species without the aluminum nitrate buffer solution present. The parameters for aluminum nitrate ($\text{Al}(\text{NO}_3)_3$) from Accornero and Marini needed slight modifications for the $\text{UO}_2(\text{NO}_3)_2/\text{HNO}_3/\text{Al}(\text{NO}_3)_3/\text{H}_2\text{O}$ system used in the extraction process during the event under consideration. The extended Pitzer model was used to calculate the equilibrium constant for extraction at steady-state and then used to predict distribution coefficients in the case of decreasing $\text{Al}(\text{NO}_3)_3$ buffer solution concentrations that led to the accident. Finally, the equilibrium constant was modified to determine the stage-wise distribution based on the uranium mass balance.

TABLE OF CONTENTS

ABSTRACT.....	iii
LIST OF FIGURES.....	v
LIST OF TABLES.....	vii
ACKNOWLEDGEMENTS.....	viii
Chapters	
1 INTRODUCTION.....	1
1.1 Background and Motivation.....	1
1.2 Process Model and Accident Background.....	4
1.3 Literature Review.....	11
2 MODEL AND THEORY.....	15
2.1 Model Development.....	15
3 EQUILIBRIUM DISTRIBUTION DURING ACCIDENT.....	32
3.1 Introduction.....	32
3.2 Steady-state Model.....	32
4 STAGE-WISE DISTRIBUTION	41
4.1 Introduction.....	41
4.2 Stage-wise Model.....	41
5 Conclusions.....	53
REFERENCES.....	55

LIST OF FIGURES

Figure	Page
1.1. Fuel pellet.....	2
1.2. Column and feed tank diagram.....	5
1.3. Detailed unit operation layout.....	6
1.4. Uranium distribution during normal conditions.....	9
1.5. Uranium distribution during accident.....	10
1.6. Pseudo-equilibrium constant distribution.....	12
2.1. Pitzer and OLI model for $\text{UO}_2(\text{NO}_3)_2$ activity coefficient for ternary system.....	22
2.2. Pitzer and OLI model for $\text{UO}_2(\text{NO}_3)_2$ activity coefficient for quaternary system.....	23
2.3. Correlation between Pitzer and OLI simulation for $\text{UO}_2(\text{NO}_3)_2$	24
2.4. Correlation between Pitzer and OLI simulation for HNO_3	25
2.5. Correlation between Pitzer and OLI simulation for $\text{Al}(\text{NO}_3)_3$	26
2.6. Correlation between Pitzer and OLI simulation for $\text{UO}_2(\text{NO}_3)_2$ modified.....	28
2.7. Correlation between Pitzer and OLI simulation for HNO_3 modified.....	28
2.8. Correlation between Pitzer and OLI simulation for $\text{Al}(\text{NO}_3)_3$ modified.....	29
2.9. Pitzer and OLI model for $\text{UO}_2(\text{NO}_3)_2$ activity coefficient modified.....	30
2.10. Pitzer and OLI model for $\text{Al}(\text{NO}_3)_3$ activity coefficient modified.....	31
3.1. Distribution as a function of $\text{Al}(\text{NO}_3)_3$	39
4.1. Stage-wise counter-current extraction.....	43

4.2. Organic phase stage-wise distribution for normal conditions.....	47
4.3. Aqueous phase stage-wise distribution for normal conditions.....	48
4.4. Organic phase stage-wise distribution during upset conditions.....	51

LIST OF TABLES

Table	Page
1.1. Uranium distribution as a function of $\text{Al}(\text{NO}_3)_3$ and HNO_3 concentration.....	7
1.2. $\text{Al}(\text{NO}_3)_3$ concentration leading up to accident.....	8
2.1. OLI simulation of activity coefficients for ternary system.....	19
2.2. Hlushak et al. Pitzer parameters.....	20
4.1. Boundary conditions for scrubbing column.....	45
4.2. Stage-wish concentration and uranium transferred.....	46
4.3. Uranium extracted during accident at steady-state.....	52

ACKNOWLEDGEMENTS

I would like to thank my advisor, Dr. Terry Ring, for choosing me for this project and his support throughout my studies both in and outside of school. I would also like to thank my committee members Dr. Geoff Silcox and Dr. John McLennan as well as the graduate advisor Dr. Misha Skliar.

A very large amount of gratitude is due to my parents and grandparents for their support in my undergraduate studies that has allowed me to avoid the financial burden of most students who have recently graduated.

I would like to thank my classmates Eric Brauser, Ethan Hecht, Josh Sewell and Palash Panja for working together on homework and class projects. Additionally, I would like to thank my classmates from my undergraduate studies Luke Andriano, Michael Reinig, Lee Stevens and Matthias Young for their help at MU and encouragement to attend graduate school. I am confident that no group of chemical engineering students has had more productive conversations at Starbucks than us. I would also like to thank Daniel Givan for some competition outside of the classroom that has carried over into our academic careers.

CHAPTER 1

INTRODUCTION

1.1 Background and Motivation

The purpose of nuclear fuel reprocessing is to separate unused uranium²³⁸ from the fission products created during nuclear reactions. Only 3% of the uranium²³⁸ is used during the power generation process. Until 1976 fuel reprocessing occurred in the United States at which time President Gerald Ford signed a presidential directive that indefinitely suspended this practice. On April 7, 1977, President Jimmy Carter banned the reprocessing of spent nuclear fuels due to nuclear proliferation concerns effectively ending research in the area in the United States.

The nuclear fuel cycle includes mining uranium oxide and converting it to uranium hexafluoride for enrichment. It is then reduced back to its oxide form and made into fuel pellets to be used in the reactor. A typical fuel pellet is shown in Figure 1.1. During the reaction the amount of uranium²³⁸ is reduced through burn-up, but at the same time uranium²³⁸ absorbs neutrons to produce plutonium. After the irradiated fuel is discharged it contains both plutonium and unused uranium which can be separated and blended to form a mixed oxide or MO_x fuel.



Figure 1.1 A typical uranium oxide fuel pellet from a nuclear reactor sent to a reprocessing unit

The nuclear fuel cycle was developed during World War II as a means of producing either plutonium or uranium weapons. After the war, the first site built to recover plutonium from irradiated fuel was in Hanford, Washington. While this site accomplished the objective of recovering plutonium, all other process streams were sent to waste. The first solvent extraction systems were the REDOX and BUTEX processes, which were a large improvement over the Hanford site but still had drawbacks such as wasted aluminum nitrate and fire hazards.

The PUREX (Plutonium and Uranium Recovery and Extraction) process using tributyl phosphate as the extractant was developed at the Savannah River site in Georgia around 1955. This process reduced waste volumes by utilizing recoverable nitric acid as the salting out agent. A combination of the REDOX and PUREX process was developed at Idaho National Lab around 1956 to reprocess the high burn-up fuels from naval reactors.

Spent reactor fuel contains large amounts of α -, β -, and γ -radiation from radioactive decay. The half-lives of these species can be up to thousands of years. However, shorter lived isotopes with half-lives of only a few days are also present. By storing the nuclear waste prior to the reprocessing step, the cost of shielding can be reduced through the decay of these shorter lived isotopes.

In the PUREX process plutonium²³⁹ is purified leading to homeland security concerns. More recent processes have focused on co-extraction of plutonium with uranium to avoid this potential hazard. The aim of this paper is to investigate, from a forensics standpoint, the events that occurred on October 17, 1978 at the Idaho Chemical Company, which caused a criticality event in the scrubbing column that is part of the uranium extraction unit.

To understand the events that occurred, recently developed thermodynamic models can be implemented by using both experimental and simulated results to fit the model parameters. The Pitzer model is a more rigorous model than the original reports used that takes into account interaction parameters of all species in the system in addition to the ionic strength.

By developing an unsteady-state model for the extraction process a wide variety of process conditions can be tested to determine their affects on the uranium distribution. This information can be used during start-up and shut down of the process where feed and buffer solutions have yet to reach their steady-state value.

Additionally, these models can be used to predict the conditions that would result from different upset conditions. Recently, the events at the Fukushima Daiichi have brought to the forefront the need for dynamic models for the nuclear fuel cycle. A

thorough understanding of the process will help prevent future accidents. Since plutonium is produced through the PUREX process there are also several homeland security concerns. A better understanding of criticality accidents can help to design plants that prevent these disasters.

1.2 Process Model and Accident Background

During nuclear fuel reprocessing uranium oxide fuel pellets are dissolved in a nitric acid solution to produce UO_2^{2+} and NO_3^- according to the reaction,



A simple diagram of the configuration used at the Idaho Chemical Plant for uranium extraction is shown in Figure 1.2 while a more detailed diagram showing subsequent settlers and evaporators is shown in Figure 1.3.

To separate the unused uranium, the solution is sent to an extraction column (G-111) which removes fission products in the aqueous phase while $\text{UO}_2(\text{NO}_3)_2$ transfers to the organic solvent, typically tributyl phosphate in a nonpolar diluent such as dodecane. To further ensure that all of the fission products have been removed the organic product containing the $\text{UO}_2(\text{NO}_3)_2$ is sent to a second scrubbing unit (H-100). This column removes the residual fission products and recycles a small amount of $\text{UO}_2(\text{NO}_3)_2$ into the aqueous phase.

During normal operation only a small amount and concentration of $\text{UO}_2(\text{NO}_3)_2$ is taken up by the aqueous phase, typically around 0.1 grams U/L. The organic product from the scrubbing column H-100 contains around 0.9 grams U/L. The aqueous stream

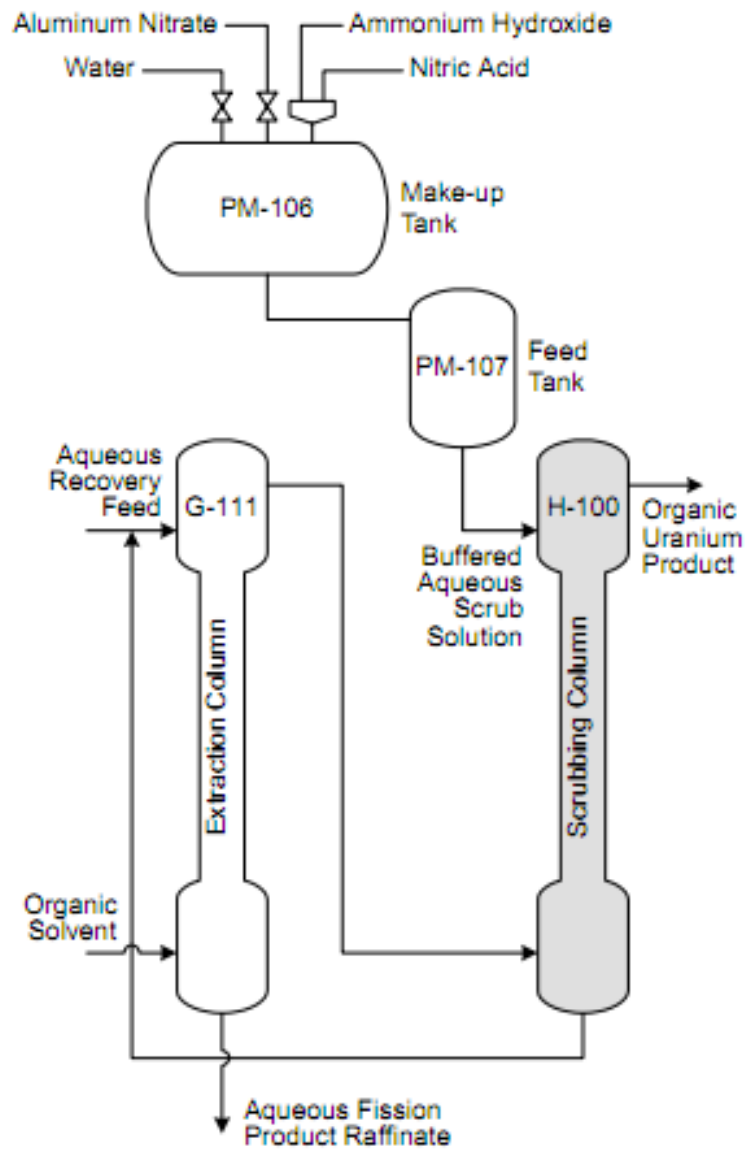
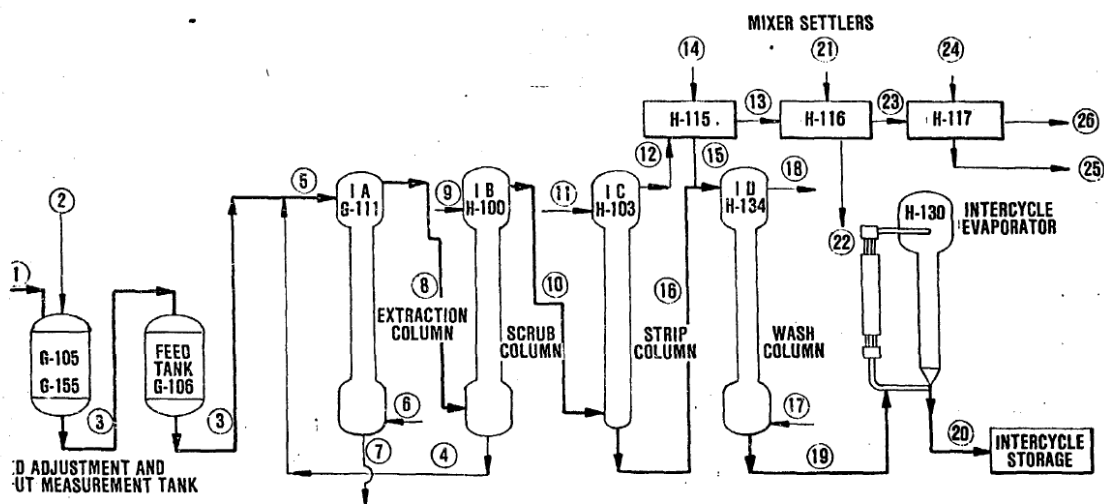


Figure 1.2. The uranium extraction section of the PUREX process operating at the Idaho Chemical Plant consisting of an extraction column, scrubbing column as well a make-up and feed tanks for the aqueous buffer solution



ACC-A-1432

Figure 1.3. Detailed schematic of the first solvent extraction cycle during the PUREX process operating at the Idaho Chemical Processing Plant from the accident report. Criticality event occurred at the base of column H-100.

leaving the scrubbing column is recycled to the extraction column G-111 which closes the loop on $\text{UO}_2(\text{NO}_3)_2$ contained in the aqueous phase.

The distribution coefficient of uranium is defined as,

$$D = \frac{[\text{UO}_2(\text{NO}_3)_2 \cdot 2\text{TBP}]_{\text{organic}}}{[\text{UO}_2^{2+}]_{\text{aqueous}}} \quad (1.1)$$

To ensure that the scrubbing column has a high distribution coefficient for $\text{UO}_2(\text{NO}_3)_2$ a buffer solution of 0.1 M HNO_3 and 0.75 M $\text{Al}(\text{NO}_3)_3$ is added to the column. The buffer solution is supplied via feed tank PM-107 which is fed by the make-up tank PM-106. Each component of the buffer solution is supplied through a separate line to the make-up tank. The distribution is a function of both sources of the nitrate ion concentration as shown in Table 1.1.

During the accident a leak in the valve supplying $\text{Al}(\text{NO}_3)_3$ caused its concentration inside the column to drop significantly from 0.7 M on September 15th to 0.08 M on October 18th. A list of the calculated $\text{Al}(\text{NO}_3)_3$ concentrations from the accident report in the month leading up to the event is shown in Table 1.2.

Table 1.1. Distribution coefficient for scrubbing column H-100 as a function of $\text{Al}(\text{NO}_3)_3$ and HNO_3 concentration with 5% tributyl phosphate

$\text{Al}(\text{NO}_3)_3$ (M)	HNO_3 (M)	Distribution Coefficient ($\text{gL}^{-1} \text{ U org} / \text{gL}^{-1} \text{ U, aq}$)
0	0	0.003
0	0.25	0.05
0.5	0	1.2
0.5	0.25	1.9
1	0	13
1	0.25	15

Table 1.2. Calculated aluminum nitrate concentration supplied to column H-100 in the month leading up to the accident showing the affect of the leaking valve.

Date	Aluminum Nitrate (M)
9/15	0.7
6/19	0.7
9/18	0.66
9/19	0.62
9/23	0.56
9/26	0.50
9/27	0.43
10/1	0.31
10/4	0.25
10/14	0.10
10/16	0.09
10/17	0.08

Additionally, the strip chart used to record the concentration had run out of paper and was not replaced until after the accident. The level of experience of the operators had dropped significantly in the two years leading to the accident. There was a density alarm on the $\text{Al}(\text{NO}_3)_3$ supply shown on the plant drawings, but this alarm had never actually been installed.

The leakage of $\text{Al}(\text{NO}_3)_3$ caused the distribution coefficient to decrease significantly causing the concentration of $\text{UO}_2(\text{NO}_3)_2$ in the aqueous recycle stream, which returns to G-111, to increase leading to an accumulation in the bottom of column H-100. The typical uranium distribution based on the dimensionless active column height is shown in Figure 1.4.

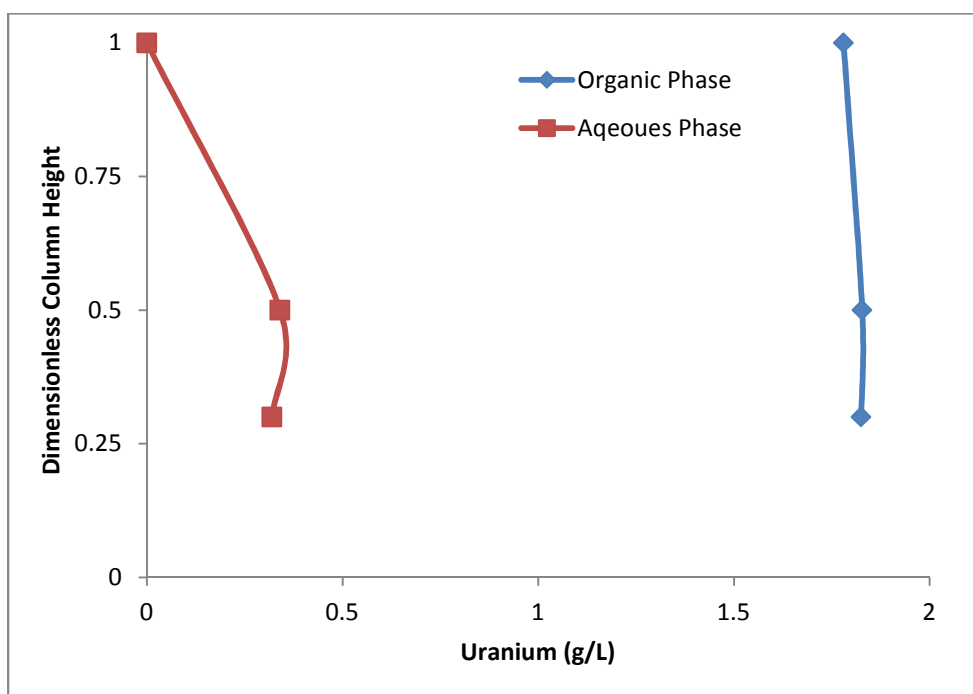


Figure 1.4. Uranium distribution in g/L based on H-100 dimensionless active column height during normal operation showing the preferential distribution of uranium into the organic phase.

At the time of the accident it was estimated that 21-22 g U/L were present in the bottom of the column. The distribution during the accident throughout the column based on the report⁶ is shown in Figure 1.5. The plant was evacuated after radiation alarms were set off. The concentration during the criticality event was determined from radiation sensors in the plant as well as analysis of radiation present during the subsequent clean up. The accident report states that there were 2.74×10^{18} measured fissions. Fortunately, no personnel were injured and no permanent equipment damage occurred.

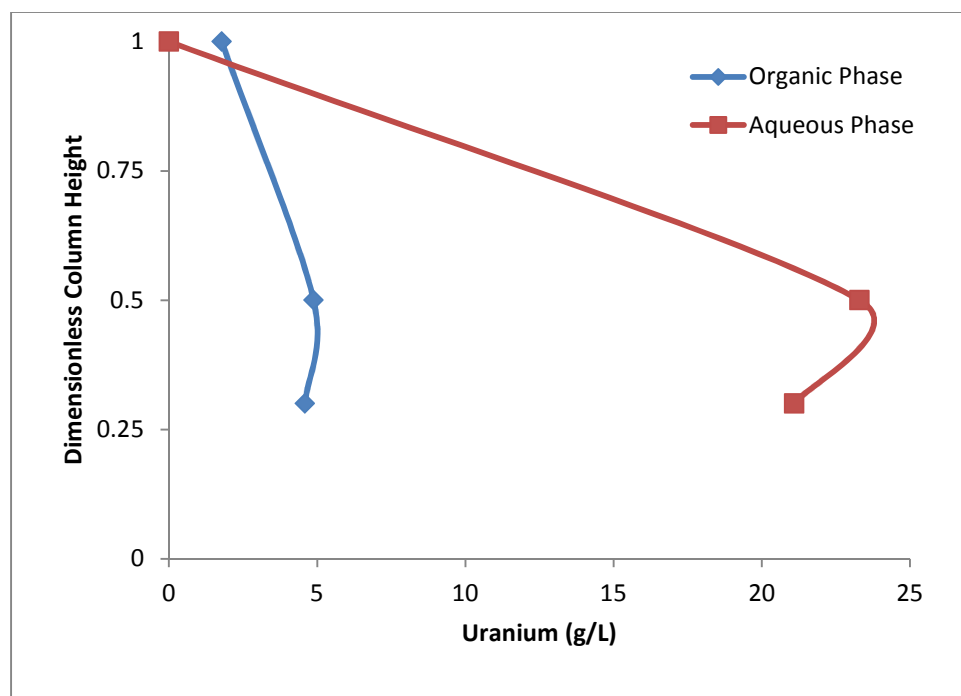


Figure 1.5. Distribution of uranium during criticality event of October 17, 1987. Maximum uranium concentrations reached 21-22 g U/L at the base of column H-100.

1.3 Literature Review

To be able to make accurate predictions of phase equilibrium present in the extraction column a fundamental understanding of the thermodynamics governing the process is needed. At the time of the accident and during the subsequent investigations this fundamental understand was not present. Simple empirical models were developed by Horner and Groenier such as the one shown in Figure 1.6. These models used a pseudo-equilibrium constant, or K'_u , that had embedded activity coefficients and they were only a function of ionic strength. An example of the correlation for the pseudo-equilibrium constant given in these models is,

$$K'_u = 12.22 + 3.810\mu - 4.798\mu^2 + 2.477\mu^3$$

where the subscript represents the constants fitted for the uranium distribution. These models were basically empirical fits to extend the simple Debye-Huckel theory which is only accurate at ionic strengths below 0.1M.

These models have several drawbacks including a lack of fundamental understanding of the process from a molecular standpoint as well as only being applicable to the concentration range measured experimentally. Since these models were only a function of ionic strength, the values for the pseudo-equilibrium constant are not unique. This is due to the fact that different concentrations for $\text{UO}_2(\text{NO}_3)_2$, $\text{Al}(\text{NO}_3)_3$ and HNO_3 can all produce the same ionic strength. As noted in the graph, the value of K'_u is not constant over the ionic strengths of interest making prediction of equilibrium concentrations impossible without an accurate activity coefficient model.

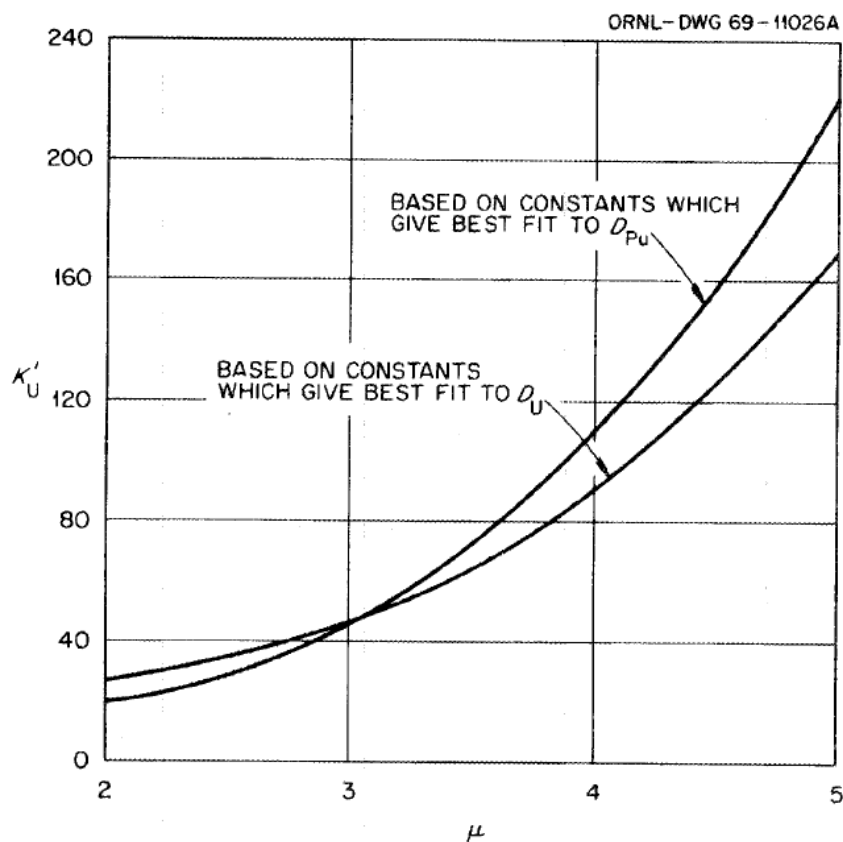


Figure 1.6. Early models using a pseudo-mass transfer coefficient, K' , with embedded activities as a function of ionic strength optimized for uranium distribution used to predict phase equilibrium during uranium extraction.

These early models were used in computer programs of the time written in FORTRAN 77 which did not amount to anything more complicated than a simple excel spreadsheet. Because of the nonuniqueness of the model parameters as many as four sets of parameters were suggested for each of the species distributions.

A major drawback of these early models is that $Al(NO_3)_3$ is not included in the system due to its removal from the scrubbing processes in plant designs after the accident. Therefore the complex affect of $Al(NO_3)_3$ on the process is not taken into

account. For the accident under investigation, this effect cannot be neglected as it was the cause the criticality event.

To correctly predict the equilibrium concentrations the activity of the NO_3^- ion must be modeled as a function of both $\text{Al}(\text{NO}_3)_3$ and HNO_3 concentrations. Current methods for calculating liquid phase activity coefficients include models such as non-random two liquid (NRTL), UNIFAC, UNIQUAC and various Pitzer models. The Pitzer model for the activity coefficient of electrolytes was first introduced in his paper in 1972 followed by a second paper in 1973 for mixed electrolytes where at least one ion was univalent. With these papers coming only five years before the accident and having only a limited number of species parameters available at the time, this model was not implemented in the report.

In May 2011, Hlushak et al. released their paper, *Description partition equilibria for the uranyl nitrate, nitric acid and water extracted by tributyl phosphate in dodecane*. They have used experimental data to determine the parameters for the extended Pitzer model in the form given by Goldberg et al. in 1988 for the ternary system $\text{UO}_2(\text{NO}_3)_2/\text{HNO}_3/\text{H}_2\text{O}$.

While this system is very close to the one present during the accident, it is still missing the parameters for $\text{Al}(\text{NO}_3)_3$. Accornero and Marini give values for the binary and ternary interaction parameters for pure $\text{Al}(\text{NO}_3)_3$. By modifying these parameters for the quaternary system $\text{UO}_2(\text{NO}_3)_2/\text{HNO}_3/\text{H}_2\text{O}/\text{Al}(\text{NO}_3)_3$ an accurate model can be obtained for the activity coefficient of each ion and neutral species in solution.

Without experimental data for the quaternary system, parameters must be determined from theory or through regression of simulated data. The OLI database can

accurately calculate activity coefficients of ions in solution even at high concentrations through the mixed solvent electrolyte model.

These activity coefficients can be used directly in the equilibrium calculation through fitting an equation for each activity coefficient as a function of its concentration. However, it is the goal of this paper to use the extended Pitzer equation to determine a rigorous thermodynamic equation that can be used to extrapolate the experimental data of Hlushak et al. to the lower concentrations that were present during the criticality accident.

CHAPTER 2

MODEL AND THEORY

2.1 Model Development

The extraction of $\text{UO}_2(\text{NO}_3)_2$ can be represented by the chemical equation,



where the equilibrium constant is given by

$$K = \frac{[\text{UO}_2(\text{NO}_3)_2 \cdot 2\text{TBP}]}{\gamma_{\text{UO}_2^{2+}} [\text{UO}_2^{2+}] \gamma_{\text{NO}_3^-}^2 [\text{NO}_3^-]^2 [\text{TBP}]^2} \quad (2.1)$$

Here γ_i represents the activity coefficient of ion i . The standard assumption of ideal behavior in the organic phase is made due to the low dielectric constant of dodecane and tributyl-phosphate.

Rearranging and using equation 1.1 the distribution coefficient is calculated as

$$D = K \gamma_{\text{UO}_2^{2+}} \gamma_{\text{NO}_3^-}^2 [\text{NO}_3^-]^2 [\text{TBP}]^2 \quad (2.2)$$

Here, $[\text{TBP}]$ is the concentration of free tributyl phosphate in the organic phase given by

$$[\text{T}]_o - 2 * [\text{UO}_2(\text{NO}_3)_2 \cdot 2\text{TBP}] \quad (2.3)$$

where $[\text{T}]_o$ is the initial concentration of tributyl phosphate. The initial concentration is calculated from

$$[\text{T}]_o = \frac{\text{volume \% TBP} * 0.973 * 1000}{266.3} \quad (2.4)$$

where 266.3 is the molecular weight of tributyl phosphate and 0.973 is the density.

Pitzer first introduced a theory for the activity coefficient of univalent ions in aqueous solutions in 1971 followed by a paper in 1972 for mixed electrolytes where one ion is univalent. Using this theory, the Gibbs excess energy of the solution is given by Goldberg as

$$\frac{G^{ex}}{RT} = n_w f(I) + 2n_w \sum_c \sum_a m_c m_a [B_{ca}(I) + E \sum_{n=1}^{N_c} C_{ca}^{(n)} I^{n-1}] \quad (2.5)$$

where a and c are anions and cations respectively, n_w is the mass of water and m_i is the molality of ion i . The ionic strength is given by $I = \frac{1}{2} \sum_i m_i z_i^2$ while E is defined as, $E = \frac{1}{2} \sum_i m_i |z_i|$ where z_i is the charge of the ion.

The summation is performed over all ions in the aqueous solution. The ternary parameter used here is referred to as C instead of Q used by Hlushak et al. to match the nomenclature used in AspenPlus in the equation for the activity coefficient of charged ions. The term N_c is the number of coefficients used in the C term. This assumes that C can be described by a polynomial fit. A value of $N_c = 1.0$ gave sufficiently accurate results over the entire concentration range which means that the ternary interaction can be approximated by a constant.

The activity coefficient for species i is calculated by differentiating the equation for the excess Gibbs energy as a function of moles of species i ,

$$\ln \gamma_i = \frac{\partial G^{ex}/RT}{\partial n_i} \quad (2.6)$$

By combining equations 2.5 and 2.6 the activity coefficient of each neutral salt is given as,

$$\begin{aligned} \ln \gamma_{cx} = & |z_c z_x| f^\gamma + \frac{2\nu_c}{\nu} \sum_a m_a \left[B_{ca} + E \sum_{n=1}^{N_c} C_{ca}^{(n)} I^{n-1} \right] + \frac{2\nu_c}{\nu} \sum_c m_c \left[B_{cx} + \right. \\ & \left. E \sum_{n=1}^{N_c} C_{cx}^{(n)} I^{n-1} \right] + \\ & \sum_a \sum_c m_a m_c \left[|z_c z_x| B'_{ca} + \frac{\nu_x z_x + \nu_c z_c}{\nu} \sum_{n=1}^{N_c} C_{ca}^{(n)} I^{n-1} + |z_c z_x| E \sum_{n=1}^{N_c} (n-1) C_{ca}^{(n)} I^{n-2} \right] \end{aligned} \quad (2.7)$$

where ν is the stoichiometric coefficient of each ion and,

$$\begin{aligned} f^\gamma = & -A_\phi \left[\frac{I^{\frac{1}{2}}}{1+1.2I^{\frac{1}{2}}} + \frac{2}{1.2} \ln(1 + 1.2I^{\frac{1}{2}}) \right] \\ B_{cx} = & \beta_{cx}^{(0)} + \frac{2\beta_{cx}^{(1)}}{\alpha^2 I} \left[1 - (1 + \alpha I^{\frac{1}{2}}) \exp(-\alpha I^{\frac{1}{2}}) \right] \\ B'_{cx} = & \frac{2\beta_{cx}^{(1)}}{\alpha^2 I^2} \left[-1 + \left(1 + \alpha I^{\frac{1}{2}} + \frac{\alpha^2 I}{2} \right) \exp(-\alpha I^{\frac{1}{2}}) \right] \\ A_\phi = & 0.392 \text{ (for water at 25 } ^\circ\text{C)} \end{aligned}$$

In this analysis it has been assumed that the correlation parameter α is equal to 2 as in the standard assumption as well as the value used by Hlushak et al.

The activity coefficient for the neutral salt calculated from the individual ions is given by the equation

$$\ln \gamma_{cx} = \frac{\nu_c \ln \gamma_c + \nu_x \ln \gamma_x}{\nu} \quad (2.8)$$

Here, ν with no subscript represents the number of ions present in the neutral species such that

$$\nu = \nu_c + \nu_x \quad (2.9)$$

The excess Gibbs energy for each ion is calculated from the modified equation given by Pitzer in 1975 which has been simplified by assuming that the unsymmetrical mixing affects are negligible,

$$\frac{G^{ex}}{RT} = n_w \left[f(I) + \sum_i \sum_j B_{ij} m_i m_j + \frac{1}{2} \sum_i \sum_j (\sum_k m_k |z_k|) C_{ij} m_i m_j \right] \quad (2.10)$$

Here, Pitzer does not distinguish between cations and anions as in the description given by Goldberg and Hlushak et al.

The activity coefficient for each charged species can be found from differentiating equation 2.10 with respect to the number of moles of species i to give

$$\ln \gamma_{m,i} = \frac{\partial \left(\frac{G^{ex}}{RT} \right)}{\partial n_i} \quad (2.11)$$

Therefore the activity of the ion is given as

$$\ln \gamma_{m,i} = \frac{1}{2} z_i^2 f' + 2 \sum_j m_j B_{ij} + \frac{1}{2} z_i^2 \sum_j \sum_k B'_{jk} m_j m_k + \frac{1}{2} |z_i| \sum_j \sum_k C_{jk} m_j m_k + \sum_j (\sum_k m_k |z_k|) C_{ij} m_j \quad (2.12)$$

where f' is equal to f'' given by Hlushak et al.

By combining equations 2.8 and 2.12 the activity coefficients of the charges ions from the OLI simulation can be used to determine the parameters for the extended Pitzer model.

For the equilibrium equation 2.1, the values of $\gamma_{UO_2^{2+}}$ and $\gamma_{NO_3^-}$ are determined by equation 2.12 written as

$$\ln \gamma_{UO_2^{2+}} = \frac{1}{2} z_{UO_2^{2+}}^2 f' + 2 m_{NO_3^-} B_{UO_2(NO_3)_2} + \frac{1}{2} z_{UO_2^{2+}}^2 (B'_{UO_2(NO_3)_2} m_{NO_3^-} m_{UO_2^{2+}} + B'_{Al(NO_3)_3} m_{NO_3^-} m_{Al^{3+}} + B'_{HNO_3} m_{NO_3^-} m_{H^+}) + \frac{1}{2} |z_{UO_2^{2+}}| (C_{UO_2(NO_3)_2} m_{NO_3^-} m_{UO_2^{2+}} + C_{Al(NO_3)_3} m_{NO_3^-} m_{Al^{3+}} + C_{HNO_3} m_{NO_3^-} m_{H^+}) + (m_{UO_2^{2+}}^2 |z_{UO_2^{2+}}| + m_{NO_3^-} |z_{NO_3^-}| + m_{Al^{3+}} |z_{Al^{3+}}| + m_{H^+} |z_{H^+}|) * (C_{UO_2(NO_3)_2} m_{NO_3^-})$$

and

$$\ln \gamma_{NO_3^-} = \frac{1}{2} z_{NO_3^-}^2 f' + 2 (m_{UO_2^{2+}} B_{UO_2(NO_3)_2} + m_{Al^{3+}} B_{Al(NO_3)_3} + m_{H^+} B_{HNO_3}) + \frac{1}{2} z_{NO_3^-}^2 (B'_{UO_2(NO_3)_2} m_{NO_3^-} m_{UO_2^{2+}} + B'_{Al(NO_3)_3} m_{NO_3^-} m_{Al^{3+}} + B'_{HNO_3} m_{NO_3^-} m_{H^+}) + \frac{1}{2} |z_{NO_3^-}| (C_{UO_2(NO_3)_2} m_{NO_3^-} m_{UO_2^{2+}} + C_{Al(NO_3)_3} m_{NO_3^-} m_{Al^{3+}} + C_{HNO_3} m_{NO_3^-} m_{H^+}) + (m_{UO_2^{2+}}^2 |z_{UO_2^{2+}}| + m_{NO_3^-} |z_{NO_3^-}| + m_{Al^{3+}} |z_{Al^{3+}}| + m_{H^+} |z_{H^+}|) * (C_{UO_2(NO_3)_2} m_{UO_2^{2+}} + C_{Al(NO_3)_3} m_{Al^{3+}} + C_{HNO_3} m_{HNO_3})$$

To determine the appropriate values of $\beta_{ij}^{(0)}$, $\beta_{ij}^{(1)}$ and C_{ij} either the osmotic coefficient, osmotic pressure or activity coefficient of each ion in solution must be known. The OLI database simulation directly provides the activity coefficient of each ion allowing for the verification of the parameters for $\text{UO}_2(\text{NO}_3)_2$ and HNO_3 from Hlushak et al. as well as modification of the $\text{Al}(\text{NO}_3)_3$ from Accornero and Marini to match the experimental data to the simulated results.

The OLI simulation requires the amount of solvent used as well as flows of each solute. The parameters for the Pitzer model are based on the molality of the solutes therefore a basis of 55.5 moles of water, or one kilogram of water, was used throughout the simulation. A typical output for the activity coefficients of the ions from the OLI simulation is shown in Table 2.1.

In the absence of $\text{Al}(\text{NO}_3)_3$, the parameters for the ternary system $\text{UO}_2(\text{NO}_3)_2/\text{HNO}_3/\text{H}_2\text{O}$ from Hlushak et al. shown in Table 2.2 should be in agreement with the OLI simulation when the concentration of $\text{Al}(\text{NO}_3)_3$ is set to zero.

The results from the OLI simulation and the values obtained from the extended Pitzer model for the ternary system $\text{UO}_2(\text{NO}_3)_2/\text{HNO}_3/\text{H}_2\text{O}$ are shown in Figure 2.1. The standard error present in the OLI simulation is around 8%. To determine the error in the

Table 2.1. OLI database simulation of the activity coefficient of ions in solution in the system $\text{UO}_2(\text{NO}_3)_2/\text{HNO}_3/\text{Al}(\text{NO}_3)_3/\text{H}_2\text{O}$, solvent is one kilogram of water.

Component Molality			Activity Coefficient			
HNO_3	$\text{Al}(\text{NO}_3)_3$	$\text{UO}_2(\text{NO}_3)_2$	H^+	Al_3^{+}	NO_3^-	UO_2^{2+}
0.1	0.2	0.04	0.625	0.925	0.022	0.163
0.1	0.4	0.08	0.634	1.102	0.021	0.166
0.1	0.6	0.12	0.665	1.318	0.026	0.198

0.1	0.8	0.16	0.701	1.593	0.037	0.255
0.1	1	0.2	0.739	1.939	0.057	0.341

Table 2.2. Values for binary and ternary interaction parameters determined by Hlushak et al.

Parameter	UO ₂ (NO ₃) ₂	HNO ₃
$\beta_{ij}^{(0)}$	0.5104	0.1083
$\beta_{ij}^{(1)}$	1.0677	0.4165
C_{ij}	-0.016552	-0.00201

Pitzer parameters the values of $\beta_{ij}^{(0)}$, $\beta_{ij}^{(1)}$ and C_{ij} were varied to determine at how sensitive these values were. Within 5% of the literature values the results were similar whereas the deviation became notice outside of this range. It can be seen that there is a close agreement between the OLI results and those predicted by the Pitzer model.

The addition of Al(NO₃)₃ to the system has a drastic affect on the ionic strength of the solution and therefore increases significantly the non-ideal behavior of the system. The nitrate concentration of the system prior to the introduction of Al(NO₃)₃ is almost solely a function of nitric acid due to the very low concentration of UO₂(NO₃)₂. During steady-state operations at the Idaho Chemical Plant, the concentration of Al(NO₃)₃ was around 0.75 M which corresponds to a nitrate concentration of 2.25 M. This causes the activity coefficient of the nitrate in solution to be a strong function of both Al(NO₃)₃ and HNO₃. Results for the activity coefficient of UO₂(NO₃)₂ as function of its concentrations As can be seen from comparing Figures 2.1 and 2.2 the values of the activity coefficient in the presence of Al(NO₃)₃ are significantly different. As a first approximation the values from Accornero and Marini were used for the Al(NO₃)₃ parameters. However, this

did not produce a satisfactory correlation between the OLI simulation and the Pitzer model. The values for the activity coefficient from the OLI simulation are graphed against those from the Pitzer model using the parameters for pure $\text{Al}(\text{NO}_3)_3$ in Figures 2.3 - 2.5 showing the poor agreement between the model and theory. When model and theory are in agreement the points will be linear on a 45 degree slope that intersects the origin.

From Figures 2.3, 2.4 and 2.5 it can be seen that the error in the activity coefficients is as large as 400%.

Due to the close agreement between the Pitzer model and the OLI simulation for the ternary system as seen in Figure 2.1, it was assumed that the parameters from Hlushak et al. could be used in the quaternary system as well for the species $\text{UO}_2(\text{NO}_3)_2$ and HNO_3 . This leaves the parameters for $\text{Al}(\text{NO}_3)_3$ to be modified to bring the model into agreement the OLI simulation.

The values for $\beta_{\text{Al}(\text{NO}_3)_3}^{(0)}$, $\beta_{\text{Al}(\text{NO}_3)_3}^{(1)}$ and $C_{\text{Al}(\text{NO}_3)_3}$, were optimized by minimizing the error between the OLI simulation results and the Pitzer model by varying these parameters using the values of Accornero and Marini as a starting point for the iteration. It was observed that the parameter $C_{\text{Al}(\text{NO}_3)_3}$ has a competing affect for the activity coefficient of $\text{Al}(\text{NO}_3)_3$ and $\text{UO}_2(\text{NO}_3)_2$. While a slightly negative value gave a close correlation for the activity coefficient of $\text{Al}(\text{NO}_3)_3$, a slightly positive value produced a good agreement for $\text{UO}_2(\text{NO}_3)_2$.

Therefore, a value of zero was chosen for $C_{\text{Al}(\text{NO}_3)_3}$ which is equivalent to the B-Pitzer model where only values of $\beta_{\text{Al}(\text{NO}_3)_3}^{(0)}$, $\beta_{\text{Al}(\text{NO}_3)_3}^{(1)}$ are used. The Microsoft Excel

solver analysis tool was used to minimize the difference between the calculated values

and the OLI simulation and good agreement was found for values of $\beta_{Al(NO_3)_3}^{(0)} = 0.78 \pm$

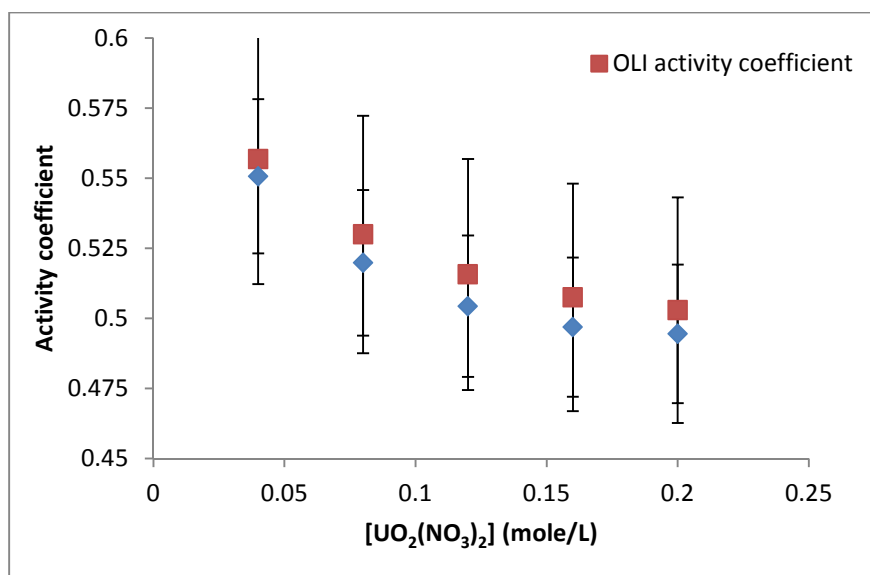


Figure 2.1 Activity coefficients for UO₂(NO₃)₂ as a function of its concentration from the Pitzer model using the parameters given by Hlushak et al. and for the OLI simulation in the ternary system UO₂(NO₃)₂/HNO₃/H₂O

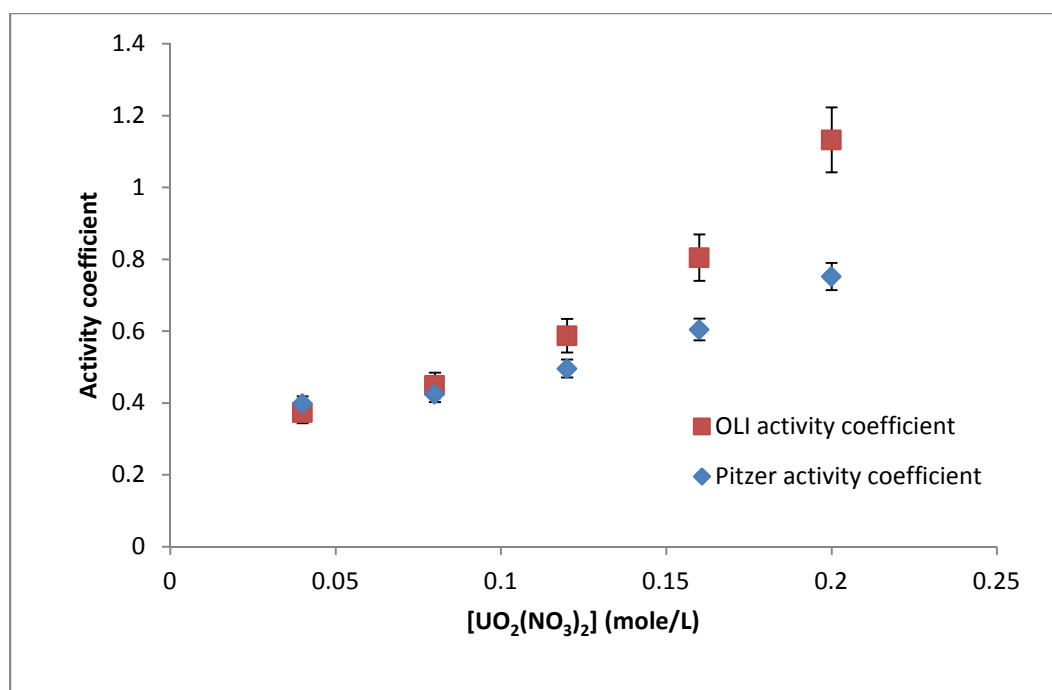


Figure 2.2. Activity coefficients for $\text{UO}_2(\text{NO}_3)_2$ as a function of its concentrations from the OLI database simulation for the quaternary system $\text{UO}_2(\text{NO}_3)_2/\text{HNO}_3/\text{Al}(\text{NO}_3)_3/\text{H}_2\text{O}$

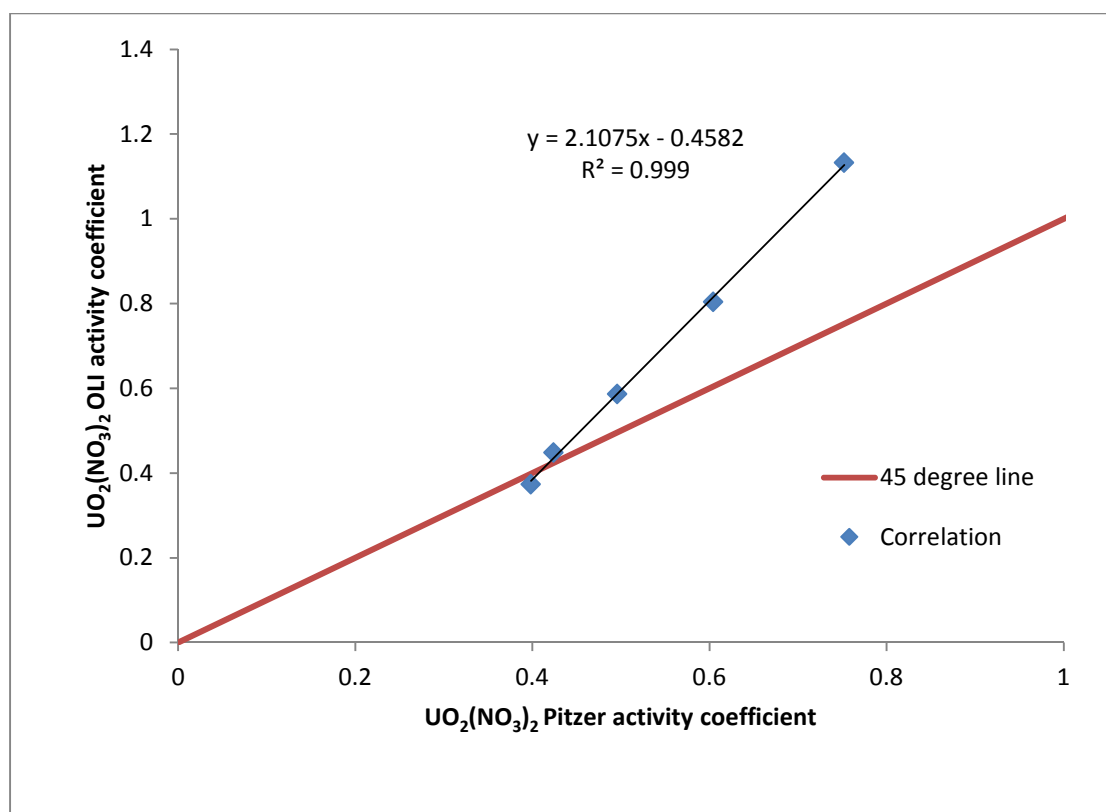


Figure 2.3. Correlation between Pitzer parameters using pure $\text{Al}(\text{NO}_3)_3$ parameters for $\text{UO}_2(\text{NO}_3)_2$ given by Accornero and Marini compared to the OLI database simulation for the quaternary system $\text{UO}_2(\text{NO}_3)_2/\text{HNO}_3/\text{Al}(\text{NO}_3)_3/\text{H}_2\text{O}$

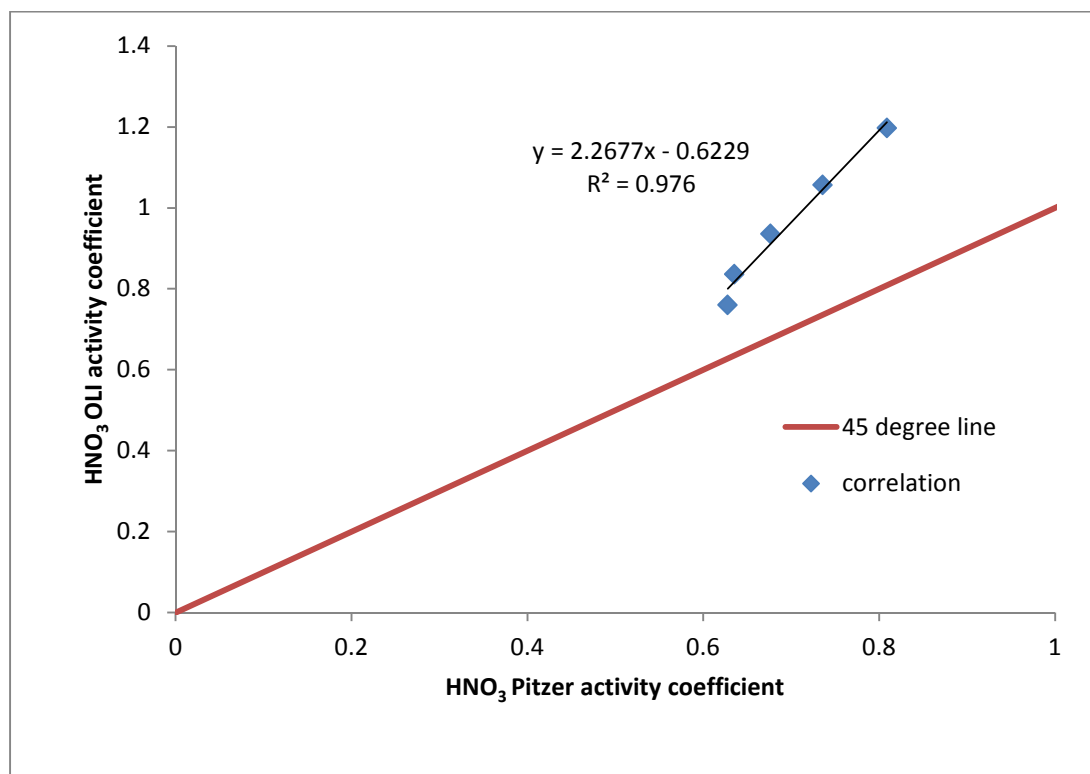


Figure 2.4. Correlation between Pitzer parameters using pure Al(NO₃)₃ parameters for HNO₃ given by Accornero and Marini compared to the OLI database simulation for the quaternary system UO₂(NO₃)₂/HNO₃/Al(NO₃)₃/H₂O

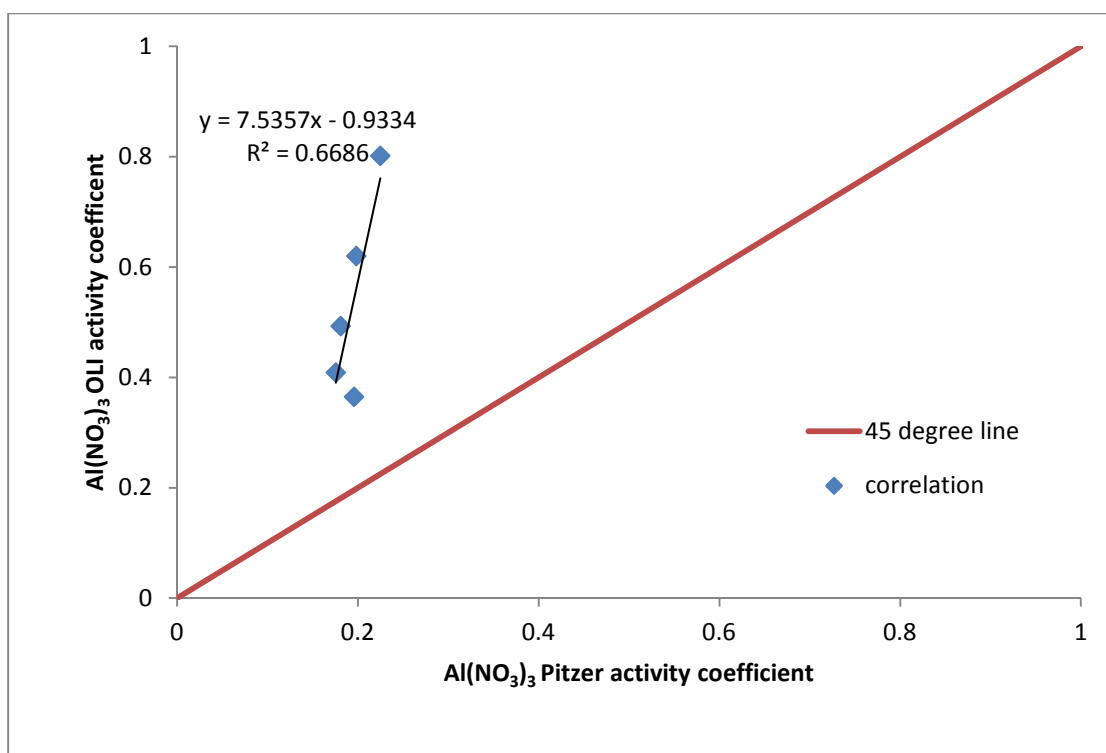


Figure 2.5. Correlation between Pitzer parameters using pure $\text{Al}(\text{NO}_3)_3$ parameters for $\text{Al}(\text{NO}_3)_3$ given by Accornero and Marini compared to the OLI database simulation for the quaternary system $\text{UO}_2(\text{NO}_3)_2/\text{HNO}_3/\text{Al}(\text{NO}_3)_3/\text{H}_2\text{O}$

0.04 and $\beta_{Al(NO_3)_3}^{(1)} = 2.5 \pm .13$ which are relatively close to the parameters for pure $Al(NO_3)_3$. The deviation reported is for the 5% error in the sensitivity of the fitted parameters.

Using these modified parameters for $Al(NO_3)_3$ the correlation between the OLI results and the Pitzer model are shown in Figures 2.6, 2.7 and 2.8. It can be seen that the agreement, while not perfect, is much closer than using the pure component parameters.

Using these parameters the activity coefficient of the neutral species $UO_2(NO_3)_2$ and $Al(NO_3)_3$ is shown as a function of their concentrations in the quaternary system in Figures 2.9 and 2.10.

Figures 2.9 and 2.10 show the agreement of the Pitzer model with the OLI simulation through the use of the modified parameters for $Al(NO_3)_3$. The extreme non-ideality created from the addition of $Al(NO_3)_3$ precludes a better fit than the one obtained. Considering these constraints, it was determined that these model parameters were sufficient to predict phase equilibrium in unsteady-state equilibrium calculations.

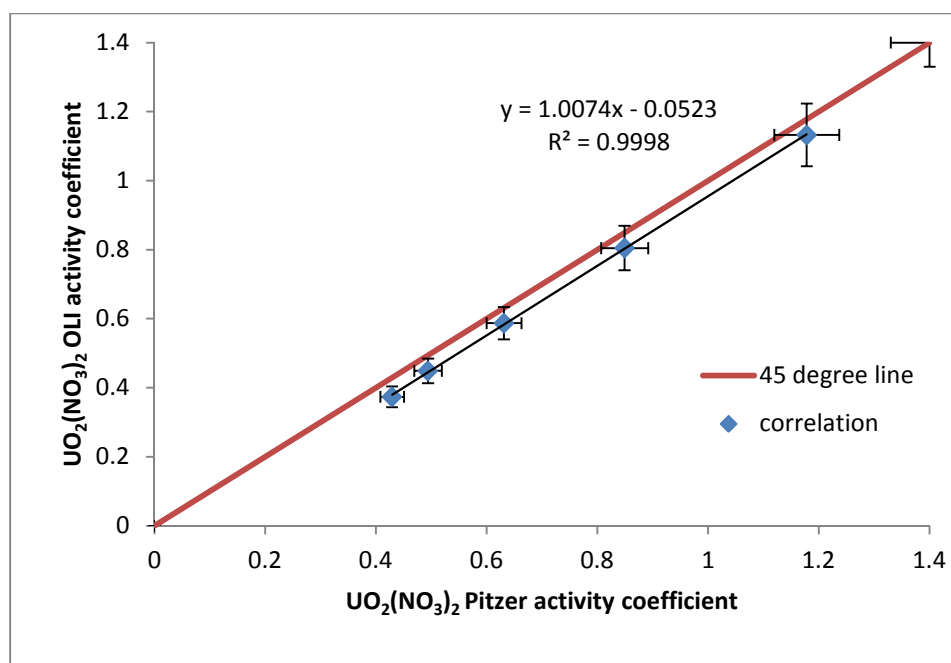


Figure 2.6. Correlation for $\text{UO}_2(\text{NO}_3)_2$ activity coefficient between Pitzer model with modified $\text{Al}(\text{NO}_3)_3$ parameters and OLI database simulation for the quaternary system $\text{UO}_2(\text{NO}_3)_2/\text{HNO}_3/\text{Al}(\text{NO}_3)_3/\text{H}_2\text{O}$

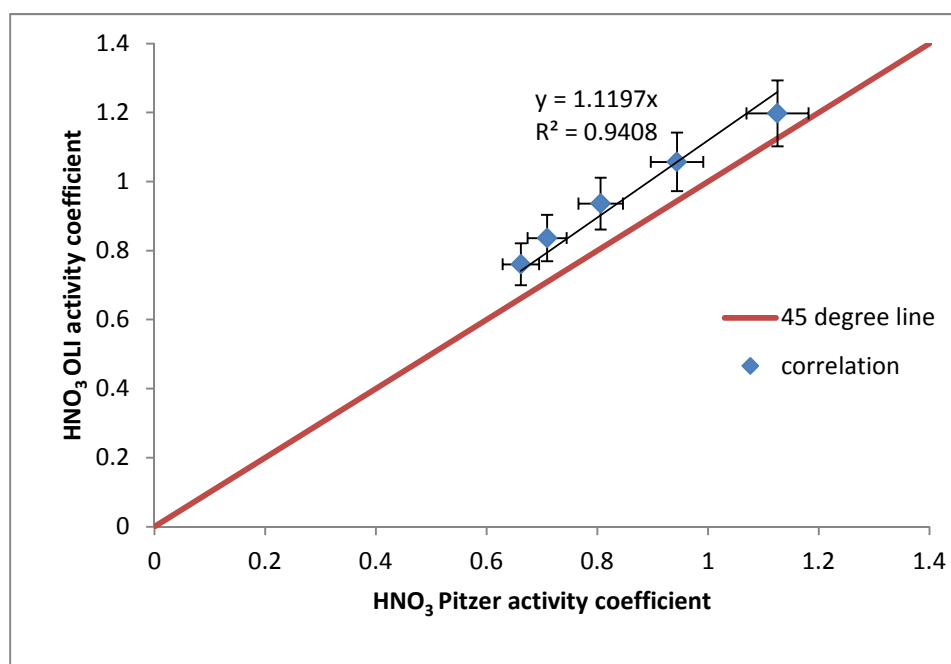


Figure 2.7. Correlation for HNO_3 activity coefficient between Pitzer model with modified $\text{Al}(\text{NO}_3)_3$ parameters and OLI database simulation for the quaternary system $\text{UO}_2(\text{NO}_3)_2/\text{HNO}_3/\text{Al}(\text{NO}_3)_3/\text{H}_2\text{O}$

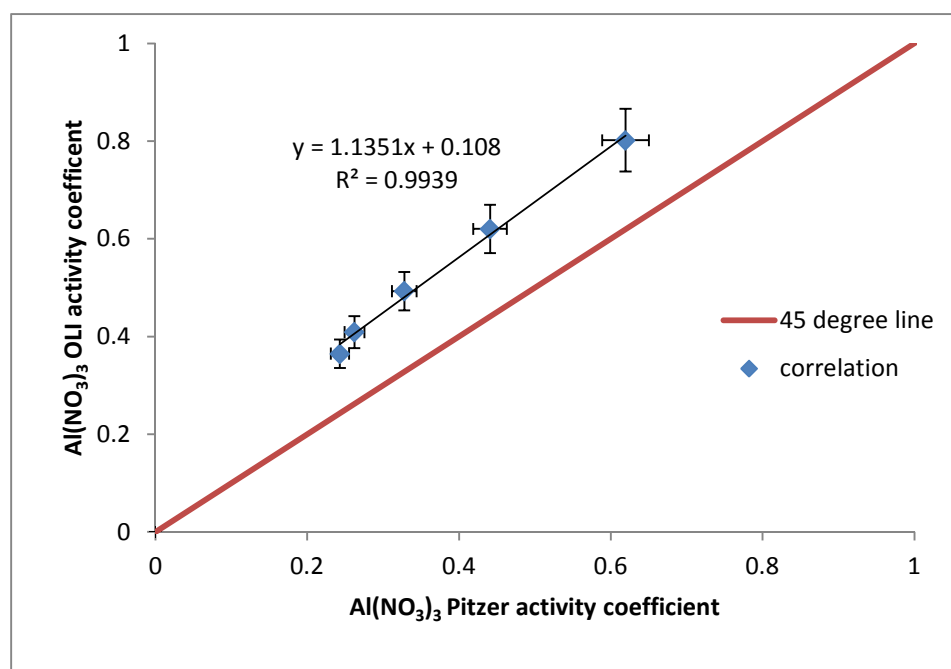


Figure 2.8. Correlation for $\text{Al}(\text{NO}_3)_3$ activity coefficient between Pitzer model with modified $\text{Al}(\text{NO}_3)_3$ parameters and OLI database simulation for the quaternary system $\text{UO}_2(\text{NO}_3)_2/\text{HNO}_3/\text{Al}(\text{NO}_3)_3/\text{H}_2\text{O}$

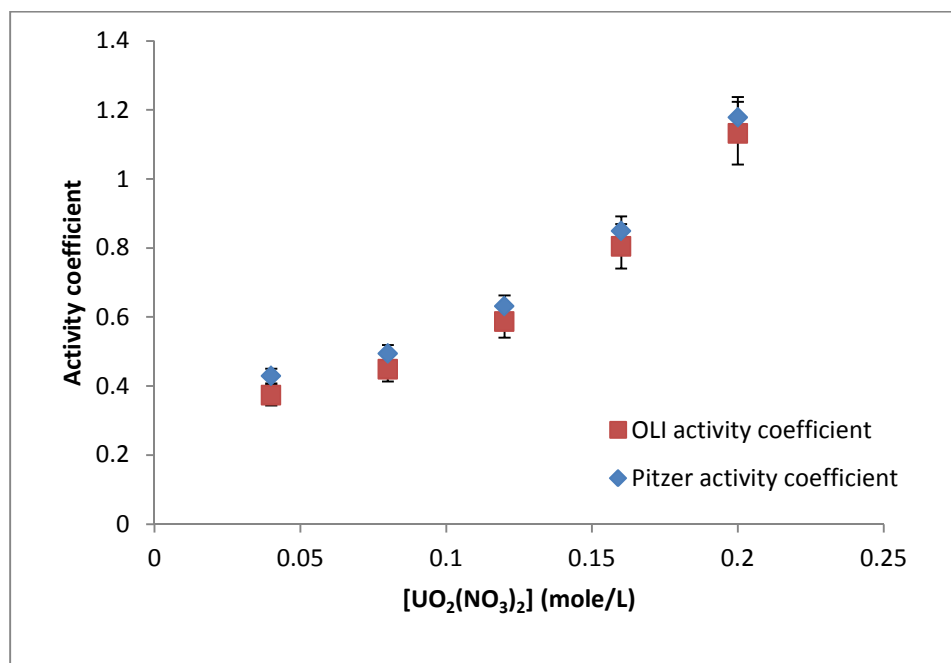


Figure 2.9. Activity coefficients for $\text{UO}_2(\text{NO}_3)_2$ as a function of its concentration for the Pitzer model using the parameters given by Hlushak et al. for $\text{UO}_2(\text{NO}_3)$ and HNO_3 and the modified parameters for $\text{Al}(\text{NO}_3)_3$

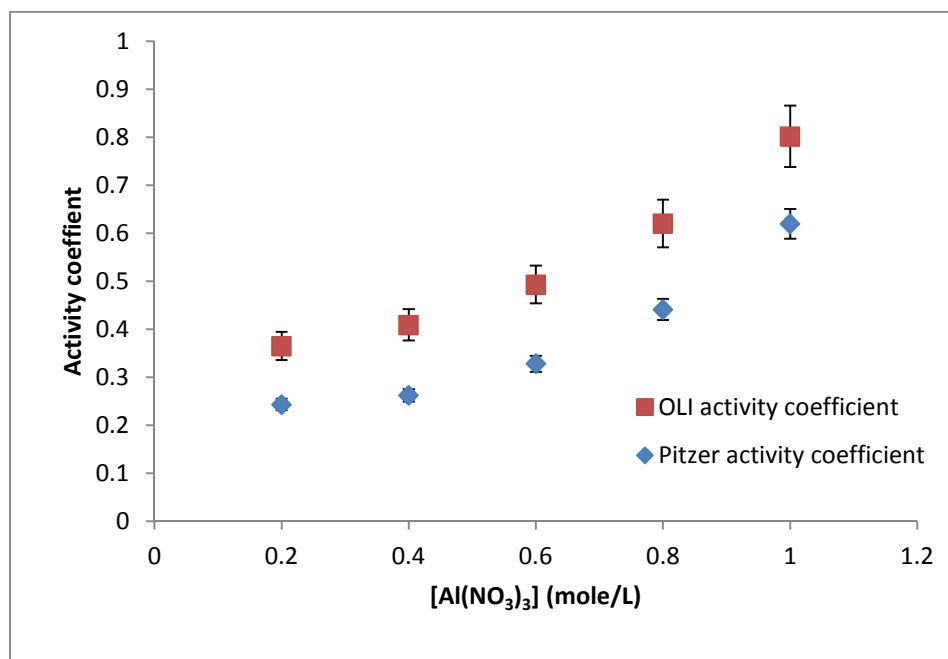


Figure 2.10. Activity coefficients for $\text{Al}(\text{NO}_3)_3$ as a function of its concentration for the Pitzer model using the parameters given by Hlushak et al. for $\text{UO}_2(\text{NO}_3)$ and HNO_3 and the modified parameters for $\text{Al}(\text{NO}_3)_3$

CHAPTER 3

EQUILIBRIUM DISTRIBUTION DURING CRITICALITY ACCIDENT

3.1 Introduction

With the appropriate parameters for the extended Pitzer equation determined over the entire concentration range of interest, the equilibrium constant for the extraction reaction can be determined at steady-state. This equilibrium constant represents the distribution for the entire column which is the value given in the report of around 0.1 g/L in the aqueous outlet stream and 0.9 g/L in the organic product. Unlike earlier models, this equilibrium constant will have a rigorous model for the activity coefficient of each ion. By determining the equilibrium constant at steady-state and using the model for the activity coefficients, the amount of uranium extracted at different nitrate ion concentrations can be calculated to model the behavior of the column leading up to the accident.

3.2 Steady-State Model

The agreement between the OLI activity coefficients and those produced with the Pitzer model using these parameters is close enough to be confident in prediction of phase equilibrium between $\text{UO}_2(\text{NO}_3)_2$ in the organic and aqueous phases. With this

model for the activity coefficients, the equilibrium equation 2.1 can be solved for the equilibrium constant, K , at steady-state.

From the Los Alamos review the concentration of uranium in the organic product from the scrubbing column H-100 is 0.9 g U/L and around 0.1 g U/L in the aqueous recycle stream. Using these values a distribution coefficient of $D = 9$ is obtained during steady state operation. The accident report presents a list of distribution coefficients shown in Table 1 that spans the entire concentration range of $\text{Al}(\text{NO}_3)_3$. However, the HNO_3 concentrations used for these distribution coefficients were either zero or 0.25 M, neither of which were present during the accident. In addition, the TBP concentration is only 5 volume percent while values between 15 and 30 are more common. It must also be noted that the operational data reports the overall distribution for the entire column⁶. Therefore, the stage-wise distribution must be determined by a different method which is developed in the following chapter.

The steady-state nitrate concentration is found by summing over all species containing NO_3^- as,

$$[\text{NO}_3^-] = [\text{HNO}_3] + 2[\text{UO}_2(\text{NO}_3)_2] + 3[\text{Al}(\text{NO}_3)_3] \quad (3.1)$$

where the coefficients in equations 3.1 represent the stoichiometric coefficient for the nitrate ion. Using the steady-state values of 0.1 M HNO_3 , 0.0004 M $\text{UO}_2(\text{NO}_3)_2$ and 0.75 M $\text{Al}(\text{NO}_3)_3$ the total nitrate concentration is 2.3504 M. To calculate the concentration of free TBP in the organic phase, the amount of uranium extracted at steady-state is subtracted from the initial TBP concentration, $[\text{T}]_0$, given by equation 2.3.

Plugging in the appropriate values for density and molecular weight of TBP and using 5 volume percent in dodecane the concentration is given by,

$$[T]_o = \frac{5 \cdot 0.973 \cdot 1000}{266.3} \quad (3.2)$$

This gives an initial concentration of 0.18 M for TBP. Given that the steady-state extraction of uranium into the aqueous phase is around 0.9 g/L the concentration of the complex $UO_2(NO_3)_2 \cdot 2TBP$ can be directly calculated as,

$$[UO_2(NO_3)_2 \cdot 2TBP] = \frac{0.9}{238} = 0.0038 \frac{\text{mole}}{\text{liter}}$$

where 238 is the molecular weight of uranium.

The value of free TBP is then calculated using equation 2.3 which gives the concentration to be used in the equilibrium equation at steady state of 0.173 M.

In the steady-state equilibrium equation the distribution coefficient or the ratio $\frac{[UO_2(NO_3)_2 \cdot 2TBP]_{organic}}{[UO_2^{2+}]_{aqueous}}$ is replaced by the known distribution during operation of about 0.9 g/L in the organic phase and 0.1 g/L in the aqueous phase. Therefore this term is,

$$D = \frac{[UO_2(NO_3)_2 \cdot 2TBP]_{organic}}{[UO_2^{2+}]_{aqueous}} = 9$$

and this value will appear in the equilibrium equation in place of those concentration terms.

With the value of $D = 9$, the calculated value of free TBP from equation 2.3, the nitrate concentration from equation 3.1 and the appropriate activity coefficients from the model the equilibrium equation is written as,

$$K = \frac{9}{\gamma_{UO_2^{2+}} \gamma_{NO_3^-}^2 [2.35]^2 [0.172]^2}$$

For these concentrations the Pitzer model gives values for the activity coefficients $\gamma_{UO_2^{2+}} = 0.174$ and $\gamma_{NO_3^-} = 0.47$. Solving this equation for the equilibrium constant

gives $K = 112.19$. This value is in close agreement with the graphs given by Horner for the ionic strength present in the system of interest.

To predict the equilibrium distribution coefficient during the criticality accident an unsteady-state model was developed that assumes steady-state is reached at several $\text{Al}(\text{NO}_3)_3$ concentrations during the month leading up to the accident. Due to the long time period over which the leak occurred as well as the high degree of mixing in the scrubbing column it is reasonable to assume that steady-state operation was reached for each $\text{Al}(\text{NO}_3)_3$ concentration. In terms of the time constants of the process it is assumed that, $\frac{\tau_{leak}}{\tau_{mixing}} \gg 1$. This allows the mass balance on the column to be solved independently without the need to couple an equation for the time dependent $\text{Al}(\text{NO}_3)_3$ concentration.

Therefore, the model will predict an exponential decrease in the distribution coefficient between two steady-state operating conditions. To determine time dependent parameters, experimental data can be used to determine the time constant of the leak assuming that $\tau_{mixing} \approx 0$. By coupling the equilibrium equation with an exponential decay term the time dependent operation can be modeled.

To determine the fresh feed of UO_2 to the process a mass balance around the extraction and scrubbing column was used. The UO_2 remaining in the aqueous phase after the scrubbing column is recycled to the extraction column. Therefore, the total concentration entering the column will be from the aqueous recycle along with the fresh feed from the organic stream. The recycle ratio for UO_2 is the amount in the aqueous phase which is returned to the column divided by the amount exiting in the aqueous phase or,

$$\text{Recycle ratio} = \frac{\text{aqueous recycle}}{\text{organic product}}$$

Plugging in the concentrations used in this system,

$$\text{Recycle ratio} = \frac{[UO_2^{2+}]_{\text{aqueous}}}{[UO_2(NO_3)_2 \cdot 2TBP]_{\text{organic}}} \quad (3.3)$$

It can be seen by inspection that the recycle ratio is the inverse of the distribution coefficient. This is a consequence of the aqueous phase exiting the scrubbing column being recycled to the organic phase leaving the extraction column instead of the aqueous phase entering the scrubbing column. It is this fact that caused the accumulation which led to the criticality event.

The only outlet flow of $UO_2(NO_3)_2$ is from the organic product of the scrubbing column. The mass balance is then given by,

$$D = \frac{[UO_2(NO_3)_2]_{\text{organic}}}{[F] + [UO_2(NO_3)_2]_{\text{aqueous}}} \quad (3.4)$$

where $[F]$ is the concentration of UO_2 in the organic feed. At the initial steady-state the values of D , $[UO_2(NO_3)_2]_{\text{organic}}$ and $[UO_2(NO_3)_2]_{\text{aqueous}}$ are known from the operational data such that $[F]$ can be solved for analytically. Using 0.9 g U/L for the organic phase and 0.1 g U/L for the aqueous phase this gives a value of $[F] = 0.003765$ M or 0.89607 g U/L. At all times in the simulation, the value of D predicts that the organic product exiting the scrubbing column contains the same amount of $UO_2(NO_3)_2$ as the fresh feed to satisfy the mass balance.

To predict the equilibrium distribution of $UO_2(NO_3)_2$ during the accident it is assumed that the concentration of $Al(NO_3)_3$ varies independently due to the leaking valve while the concentration of HNO_3 remains constant. For a given concentration of

$\text{Al}(\text{NO}_3)_3$, the unknowns are: $[\text{UO}_2(\text{NO}_3)_2]_{\text{organic}}$ and $[\text{UO}_2(\text{NO}_3)_2]_{\text{aqueous}}$, $[\text{TBP}]$, $\gamma_{\text{NO}_3^-}$ and $\gamma_{\text{UO}_2^{2+}}$. At equilibrium the calculated values must predict a distribution coefficient that meets the mass balance on $\text{UO}_2(\text{NO}_3)_2$ for the inlet and outlets as well as at each stage.

To a first approximation the nitrate concentration in $\text{UO}_2(\text{NO}_3)_2$ is a very small and can be neglected compared to that in the $\text{Al}(\text{NO}_3)_3$ and HNO_3 . During normal operations the nitrate concentration is then given by,

$$[\text{NO}_3] = 3[\text{Al}(\text{NO}_3)_3] + [\text{HNO}_3]$$

assuming complete dissociation of these ions in the aqueous phase. With the nitrate concentration calculated at progressively lower $\text{Al}(\text{NO}_3)_3$ concentrations, the distribution coefficient can be solved for in equation 2.3 with the mass balance constraint solved simultaneously.

Given the values for $[\text{NO}_3]$ and $[\text{UO}_2(\text{NO}_3)_2]_{\text{aqueous}}$, their activity coefficients are calculated as well as the amount of free TBP based on $[\text{UO}_2(\text{NO}_3)_2]_{\text{organic}}$ using equation 2.3. This procedure is repeated until the criteria for steady-state has been met. At all converged points of the simulation, the mass balance was very close to zero ensuring that steady-state had been reached and that the activities and distributions were not overly sensitive to changes in concentration.

Using this procedure a plot of the distribution coefficient as a function of $\text{Al}(\text{NO}_3)_3$ concentration is shown in Figure 3.1. The extended Pitzer model is shown along with the distribution that results from assuming ideal behavior in the liquid phase, or that the activity coefficients of the ions are equal to unity throughout the operating range during the accident.

From this plot it is seen that the distribution coefficient crosses a value of one, or where $\text{UO}_2(\text{NO}_3)_2$ is preferentially partitioned into the aqueous phase instead of the organic phase. This is equivalent to the scrubbing column acting as stripping column by removing all the $\text{UO}_2(\text{NO}_3)_2$ from the organic phase.

From Figure 3.1 it is seen that for the extended Pitzer model concentrations of $\text{Al}(\text{NO}_3)_3$ below about 0.45 M will cause UO_2 to be stripped from the organic phase to the aqueous phase or in terms of the distribution constant, $D < 1$. Assuming ideal behavior, the critical concentration is about half of this value, around 0.23 M. This reflects the variation in the activities of the NO_3^- and UO_2^{2+} varying by a factor of two over the $\text{Al}(\text{NO}_3)_3$ concentration range from typical operation to when the accident occurred. This value is in agreement with the accident report which states that under 0.5 M the distribution coefficient will be less than one.

For the Pitzer model, the distribution coefficient as a function of aluminum nitrate concentration was fitted to an exponential function,

$$D = 0.042e^{7.137[\text{Al}(\text{NO}_3)_3]}$$

The correlation for this fit was very good with an R^2 value of 0.998. For the ideal mixture, an exponential function gave an R^2 value of only 0.946. The best fit for the ideal mixture was found to be a polynomial equation, similar to analysis of Horner.

While the concentrations of $[\text{UO}_2(\text{NO}_3)_2]_{\text{organic}}$ and $[\text{UO}_2(\text{NO}_3)_2]_{\text{aqueous}}$ cannot be accurately predicted without modeling the activity coefficients, the equilibrium equation is a stronger function of nitrate concentration than activity coefficient. During normal operation the nitrate concentration is 2.35 M. At the time of the criticality accident, the

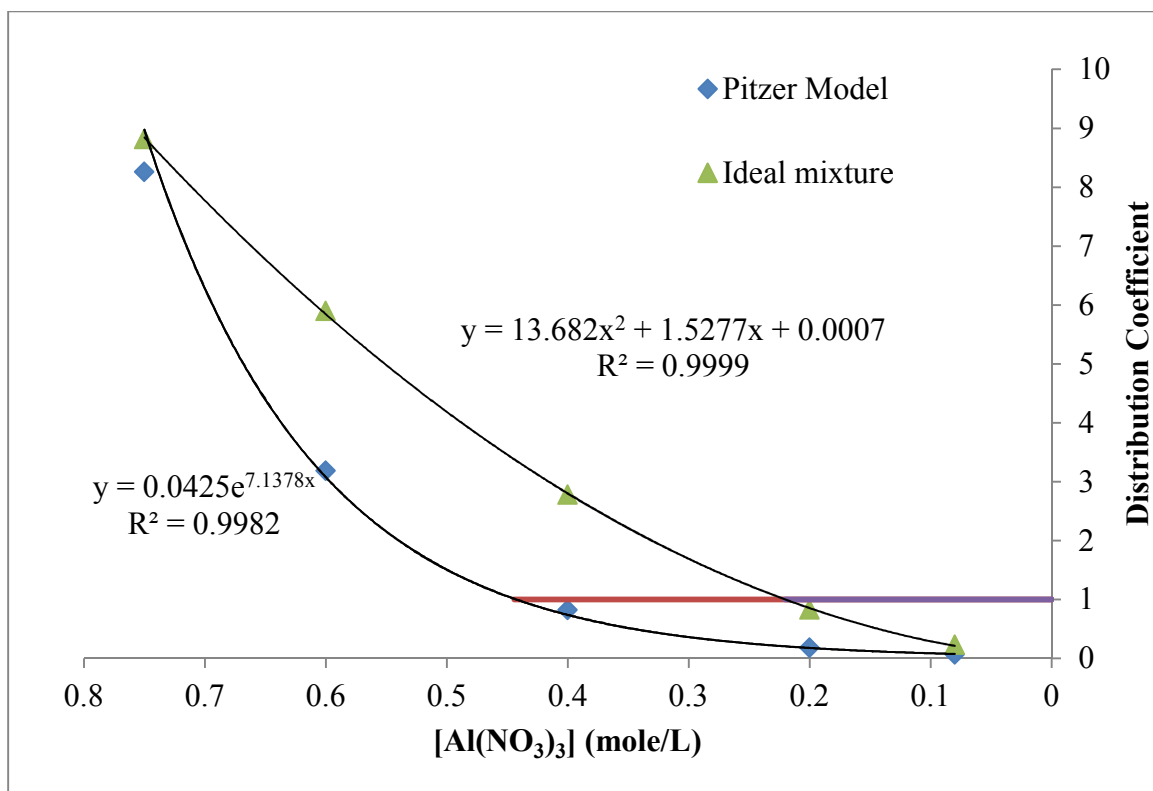


Figure 3.1. Distribution coefficient as a function of $\text{Al}(\text{NO}_3)_3$ concentration in column H-100 from the normal steady-state operation to the critically accident for the extended Pitzer model and for an ideal solution model.

nitrate concentration was only 0.34 M. Considering that the nitrate concentration in the equilibrium equation is squared, this gives a variation of almost 5.5 over the concentration range. This compares with a variation of around a factor of 2 for the activity coefficients.

Using the mass balance for uranium and the final distribution coefficient at the concentration of $\text{Al}(\text{NO}_3)_3$ present in the accident, the amount of uranium that would have accumulated in column H-100 is calculated to be slightly under 13 g U/L. The accident report reports that the number of fission events measured would correspond to a concentration of 21 – 22 g U/L which is higher than that predicted by the model. This

could be due to the concentration of $\text{Al}(\text{NO}_3)_3$ being lower than the calculated value of 0.08 M or mixing affects that caused uranium to accumulate beyond its thermodynamic equilibrium value such as settling due to its high density relative to water.

Uranium accumulating at the bottom of the column, where the accident occurred, would certainly not have been in thermodynamic equilibrium with the organic stream and buffer solution entering the top of the column due to the lack of intimate contact between the two phases. Also, the Pitzer model parameters for $\text{Al}(\text{NO}_3)_3$ are based on the fitting against the OLI simulation. Small errors in the fitted equations along with the lack of mixing could account for the difference in simulation results compared with the operational data.

Using the equation for the distribution coefficient the amount of uranium that would have accumulated when the aluminum nitrate concentration reached zero is given by the constant of the exponential function, 0.042. Using this distribution in equation 2.2 and the inlet organic concentration, the aqueous recycle would reach 0.09 M for $\text{UO}_2(\text{NO}_3)_2$ or 21.335 g U/L which is in almost exact agreement with the experimental value. From the analysis it is likely that this larger amount of uranium collected at the bottom of the column and did not come into contact with the aqueous phase entering the top of the column.

CHAPTER 4

STAGE-WISE DISTRIBUTION

4.1 Introduction

The available operational data for the scrubbing column gives an overall distribution coefficient that is the ratio of the outlet aqueous and organic phases. To determine the distribution coefficient throughout the column a procedure was developed which iteratively solves for the distribution at each stage until the overall distribution matches the experimental data. By using this stage-wise method the concentration of uranium at all points of the column can be calculated. With the concentration of uranium at each point in the column known, the model can predict at what location the criticality event would have occurred.

4.2 Stage-wise Model

In order to understand the equilibrium distribution throughout the column, a procedure was developed that used the overall distribution coefficient from the Pitzer model to match the known inlet and outlet concentrations. The equilibrium constant for the overall distribution is for the outlet flow of the organic phase from the top of the column and the aqueous phase leaving the bottom of the column. To model the counter-

current extraction, it was assumed that five equilibrium stages were appropriate to predict the distribution. Column H-100 was four feet tall which would give a theoretical stage height of 0.8 feet for five stages.

The equilibrium constant from equation 2.1 is for the overall column distribution based on the available operational data. To understand the behavior at each stage the equilibrium constant K_{stage} is calculated. This value is for streams leaving the same stage as opposed to the overall distribution for the entire column.

While there is no data for the internal distribution, an equilibrium constant for the first stage can be determined that is used throughout the column to predict the outlet concentrations. Given the known values for the overall distribution, the new stage-wise equilibrium constant can be solved for iteratively to determine what the equilibrium distribution is at each stage. A representation of the uranium transferred between stages is shown in Figure 4.1 where the vertical lines represent the stripping of material from the organic to the aqueous phase.

At each stage the amount of uranium leaving is calculated beginning with the first stage. Because the outlet of the first stage, the aqueous recycle stream, is known the aqueous outlet can be solved for given the distribution coefficient at steady-state. In turn, this is amount and concentration of uranium that is used for the inlet to the second stage. This ensures that the mass balance on uranium is satisfied at each stage throughout the column.

To begin the iteration procedure an upper bound on the equilibrium constant for the first stage can be determined by assuming that the entire amount of uranium is removed from the aqueous phase in this stage. At these conditions the organic phase

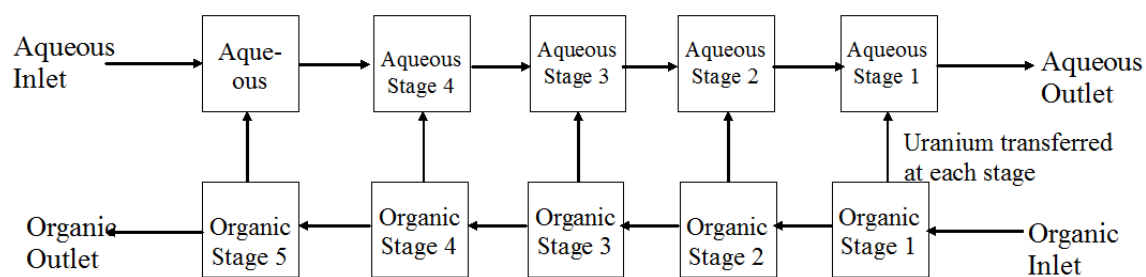


Figure 4.1. Stage-wise distribution model with organic flow on bottom and aqueous flow on top. Vertical lines show uranium being transferred between phases at each

entering the first stage would contain the fresh feed of uranium and the aqueous recycle while the stream exiting the first stage contains the steady-state outlet concentration for the entire column.

By increasing the equilibrium constant the upper bound is determined by matching the amount of uranium exiting the first stage with the amount that would transfer between the organic and aqueous phase by solving for the distribution coefficient. It was determined that a value of $K_{stage} = 131.9$ which corresponds to a distribution coefficient $D = 10.41$ cannot be exceeded. Above these values the model predicts that more uranium than is present in the aqueous exit stream can transfer in the first stage which is physically unrealistic.

Figures 1.4 and 1.5 show that the majority of the uranium is transferred near the top of the column. This is seen through the very steep line connecting the inlet aqueous feed and the concentration in the middle of the column. The section between the middle of the column and the base has an almost linear profile during normal operating conditions. Therefore, only a small amount of uranium is transferred at each stage near the bottom of the column. It is also important to remember that this scrubbing column causes uranium to be transferred from the organic phase to the aqueous phase through scrubbing even though the majority of the uranium entering and leaving the column is in the organic phase.

The slope of the concentration profile in the column is determined by modifying the equilibrium constant to match the operational data, or the boundary conditions at the inlet and outlet shown in Table 4.1.

At large equilibrium constants, approaching the limit of 131.9, the entirety of the uranium is transferred in the first stage. In this case, the model will predict negative concentrations of uranium in the subsequent stages. This means that the distribution coefficient calculated from equation 2.2 is too large. By reducing the equilibrium constant in the first stage, the distribution coefficient will also be reduced until each stage has a positive uranium concentration and meets the boundary conditions in Table 4.1.

To determine the exact value of the equilibrium constant for the first stage, the boundary condition that the inlet flow of the aqueous phase has zero concentration must be met. This stream is fed from the feed tank PM-107 which contains only the nitric acid and aluminum nitrate buffer solutions. For an equilibrium constant $K_{stage} = 131.89$ the inlet and outlet flow for the aqueous phase match the operational data and also gives the correct concentration in the outlet organic stream. The value for K_{stage} is extremely sensitive due to the steep concentration slope shown in Figure 1.4 near the aqueous inlet.

The results for the amount of uranium transferred at each stage along with the aqueous and organic concentrations using a value of $K_{stage} = 131.89$ are shown in Table 4.2.

Table 4.1. Boundary conditions for the overall distribution used to satisfy the mass balance for the stage-wise calculation procedure.

	Organic phase concentration (mole/L)	Aqueous phase concentration (mole/L)
Inlet	0.0042	0
Outlet	0.0038	0.00042

Table 4.2. Amount of uranium transferred at each stage along with concentration in organic and aqueous phase for a stage-wise equilibrium constant $K_{stage} = 131.89$ during normal operating conditions.

Stage	Uranium transferred (grams)	Organic Concentration (mole/L)	Aqueous Concentration (mole/L)
1	7.73E-06	4.1650E-03	4.000E-04
2	7.98E-05	4.1646E-03	3.996E-04
3	8.24E-04	4.1612E-03	3.962E-04
4	8.50E-03	4.1255E-03	3.605E-04
5	8.78E-02	3.7565E-03	0.000E+00

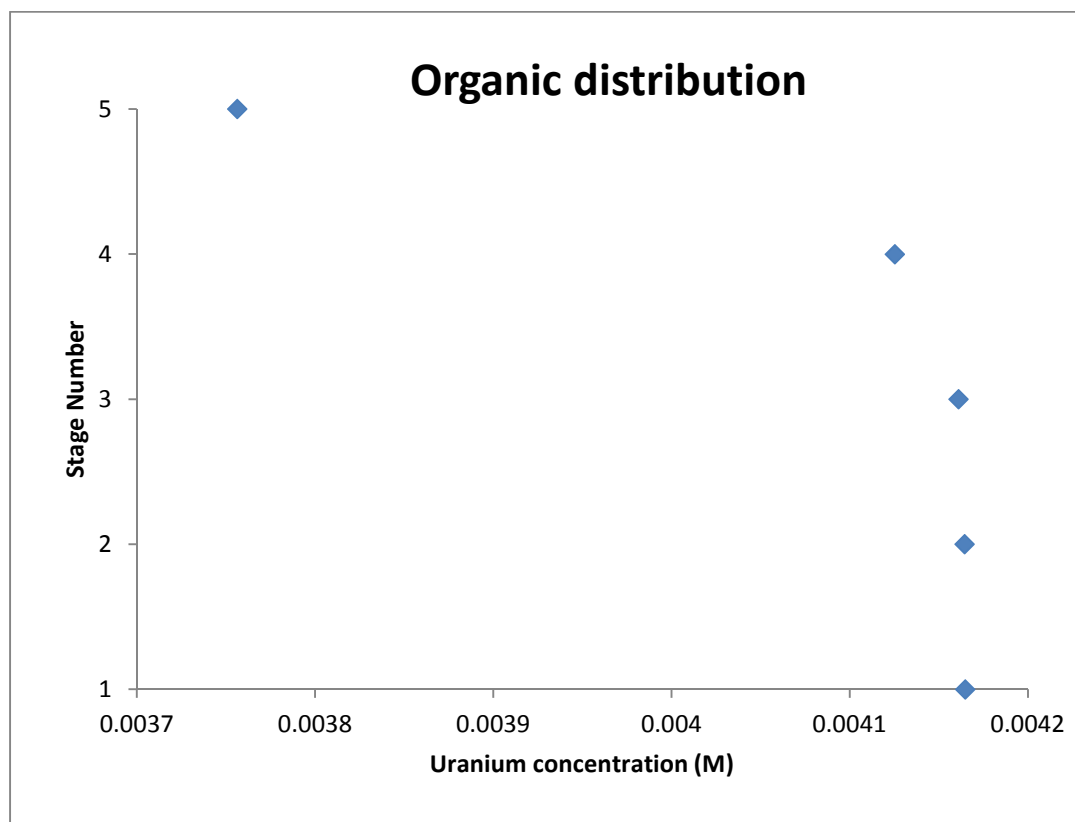


Figure 4.2. Organic phase stage-wise distribution for column H-100 during normal operating conditions using a value of $K_{stage} = 131.89$.

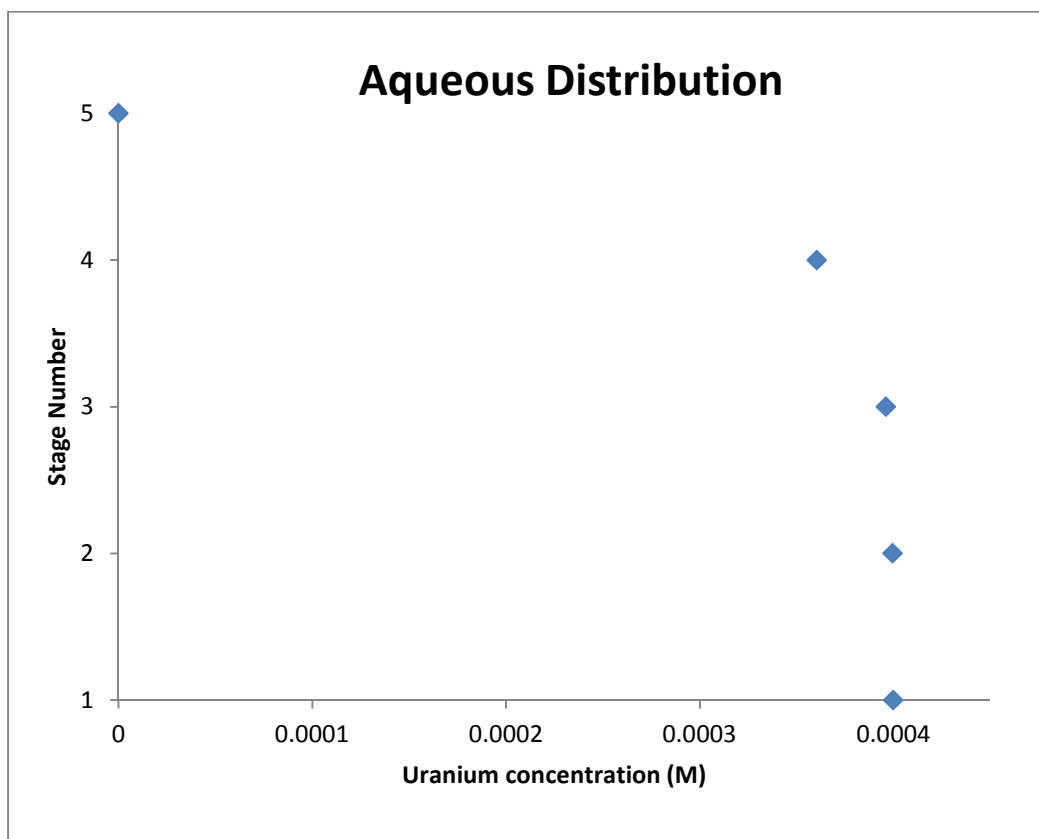


Figure 4.3. Aqueous phase stage-wise distribution for column H-100 during normal operating conditions using a value of $K_{stage} = 131.89$.

During the upset conditions that took place in the criticality accident, the concentration of nitrate in the aqueous phase was low enough that a large amount of uranium could transfer to the aqueous phase. This increased the concentration in the recycle stream to column G-111 which returned into column H-100 through the organic phase. At the time of the accident the stage-wise calculation with the given Pitzer parameters shows that the aqueous phase could continue to accept uranium beyond the amount that was entering in the organic phase. This means that the accumulating uranium was constantly being stripped from the organic phase as soon as it entered column H-100. Therefore that the amount of uranium removed from the organic phase will cause the equilibrium concentrations in the model to become negative if the system has yet to achieve steady-state as shown in Figure 4.4.

Of course, this is not a physically realistic situation and would simply correspond to all of the uranium in the organic phase transferring to the aqueous phase near the bottom of the column. This causes the slope of the aqueous distribution between the lower stages of the column and the top of the column to be very sharp. This corresponds well with Figure 1.5 which is given in the accident report showing large amounts of uranium near the bottom of the column.

The model predicts negative concentration values, or larger distribution coefficients than possible given the amount of uranium available. At the time of the accident, the alarm system and the actions of the operator caused the event to end before a final steady-state was reached. The amount of uranium transferred in each stage is found by calculating the difference in the concentrations between each stage and multiplying by the molecular weight,

$$([UO_2^{2+}]_n - [UO_2^{2+}]_{n-1}) * MW_{uranium}$$

Using the difference in the concentrations from Figure 4.4 the amount of uranium that would transfer at each stage at steady stage is shown in Table 4.3.

As mentioned before, the actual concentration of uranium at the bottom of the column could be significantly higher due to density differences and a lack of mixing. The close agreement in the shape of the stage-wise profile predicted from the model in Figures 4.2 and 4.3 compared with the available data in Figures 1.4 and 1.5 indicate that the stage-wise distribution method developed is accurate. During the accident several competing affects such as temperature fluctuations and operating pressure of the column would have caused the distribution of uranium to deviate from its thermodynamic equilibrium given by the model.

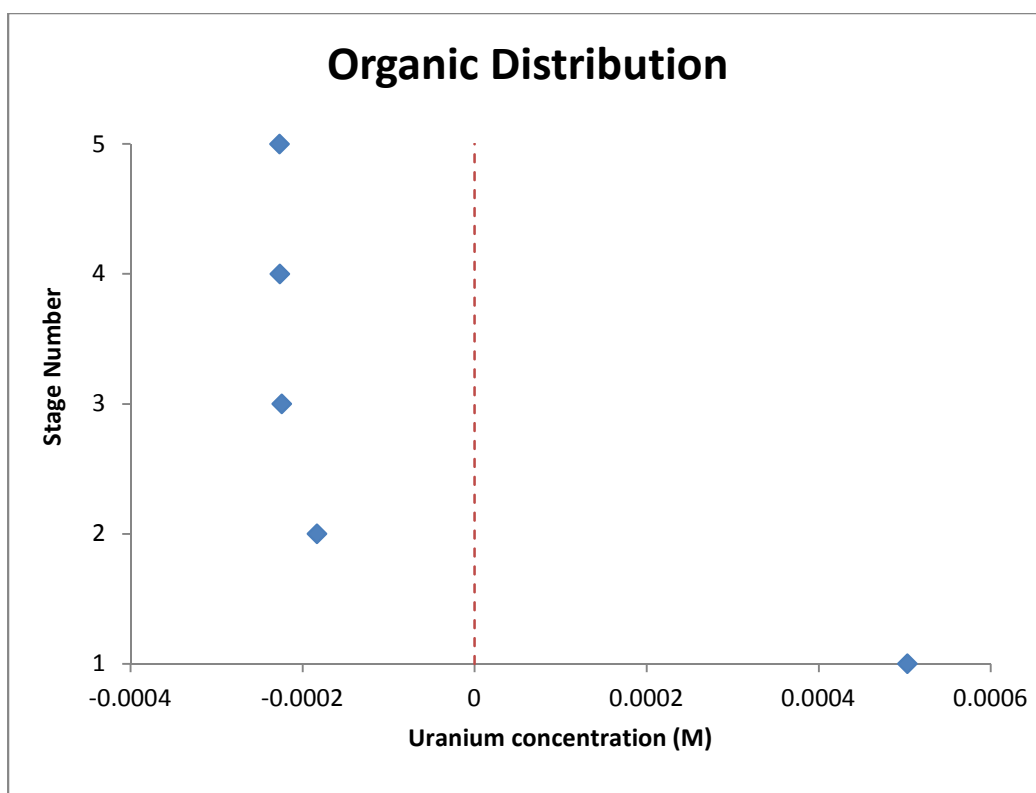


Figure 4.4. Distribution of uranium during criticality accident predicted from model. Negative values show that more uranium than was present in the organic phase can be transferred to the aqueous phase at equilibrium meaning the column was not yet operating at steady-state when the criticality accident occurred.

Table 4.3. Amount of uranium that would have transferred at each stage during the criticality accident if steady-state had been reached before the event was stopped through reduction of pressure of the column causing the flow rate to increase which led to adequate mixing in the bottom of the column.

Stage	Uranium transferred (grams)
1	12.69
2	0.163
3	0.0097
4	0.0006
5	3E-05

CHAPTER 5

CONCLUSIONS

The extended Pitzer model was applied successfully to the ternary system $\text{UO}_2(\text{NO}_3)_2/\text{HNO}_3/\text{H}_2\text{O}$ with the parameters given by Hlushak et al. at much lower $\text{UO}_2(\text{NO}_3)_2$ concentrations than present in their experimental system. However, literature values for pure $\text{Al}(\text{NO}_3)_3$ did not produce a satisfactory correlation between the Pitzer model and the OLI simulation for the quaternary system $\text{UO}_2(\text{NO}_3)_2/\text{HNO}_3/\text{Al}(\text{NO}_3)_3/\text{H}_2\text{O}$. By varying the parameters for $\text{Al}(\text{NO}_3)_3$ slightly the values $\beta_{\text{Al}(\text{NO}_3)_3}^{(0)} = 0.78 \pm 0.04$ and $\beta_{\text{Al}(\text{NO}_3)_3}^{(1)} = 2.5 \pm .13$ were determined to be appropriate for this system.

Using the parameters from Hlushak et al. along with the new parameters for $\text{Al}(\text{NO}_3)_3$, the equilibrium constant $K = 112.9$ was determined for overall distribution of the column at steady-state for several $\text{Al}(\text{NO}_3)_3$ concentrations leading up to the accident. This analysis showed that with 0.45 M $\text{Al}(\text{NO}_3)_3$ uranium will accumulate in the aqueous phase.

By modeling the column as five counter-current stages a modified equilibrium constant of $K_{\text{stage}} = 131.89$ was determined for the first stage and used throughout the column. This equilibrium constant applies to organic and aqueous phases that are in

direct contact in each stage as opposed to the value originally obtained for the overall column. The stage-wise equilibrium process was used to solve for the distribution of uranium throughout the column by satisfying the mass balance on all input and output streams. The distribution at the normal steady-state operating conditions was in close agreement with the operational data. This analysis showed that during the accident the column had yet to reach a steady-state distribution.

REFERENCES

- Accornero, M., and Marini, L., 2009. Empirical prediction of the Pitzer's interaction parameters for cationic Al species with both SiO₂(aq) and CO₂(aq): Implications for the geochemical modelling of very saline solutions. *Applied Geochemistry*, 24, 747-759.
- Casto, W. R., 1980. ICPP Criticality Event of October 17, 1978. *Nuclear Safety*, 21 (5), 648-663.
- Godfrey, W. L., Hall, J. C. and Townes, G. A. 2000. *Nuclear Reactors, Chemical Reprocessing*. Kirk-Othmer Encyclopedia of Chemical Technology.
- Goldberg, R., 1979. Evaluated activity and osmotic coefficients for aqueous solutions: bi-univalent compounds of lead, copper, manganese, and uranium. *J. Phys. Chem. Ref. Data* 8, 1005–1050.
- Gronier, W.S., 1972. Calculation of the transient behavior of a dilute-purex solvent extraction process having application to the reprocessing of LMFBR fuels. ORNL-4746.
- Hlushak, S.P., 2011. Description of the partition equilibrium for uranyl nitrate, nitric acid and water extracted by tributyl phosphate in dodecane. *Hydrometallurgy*. 109, 97-105.
- Horner, D.E., 1968. A mathematical model and a computer program for estimating distribution coefficients for plutonium, uranium, and nitric acid in extractions with tri-n-butyl phosphate. ORNL-TM-2711.
- Pitzer, K.S., 1973. Thermodynamics of electrolytes. I. Theoretical basis and general equations. *J. Phys. Chem.* 77, 268–277.
- Pitzer, K.S., 1973. Thermodynamics of electrolytes. II. Activity and osmotic coefficients for strong electrolytes with one or both ions univalent. *J. Phys. Chem.* 77 (19), 2300–2308.
- Pitzer, K.S., and Kim, J.J., 1974. Thermodynamics of electrolytes. IV. Activity and osmotic coefficients for mixed electrolytes. *J. American Chemical Society* 96, 5701-5707.